AD-A144 350 FATIGUE OF SYNTHETIC FIBERS FOR MARINE ROPE APPLICATIONS(U) MASSACHUSETTS INST OF TECH CAMBRIDGE DEPT OF MATERIALS SCIENCE AND ENGINEERING

UNCLASSIFIED M C KENNEY ET AL. APR 84 R84-2 F/G 11/5 NL

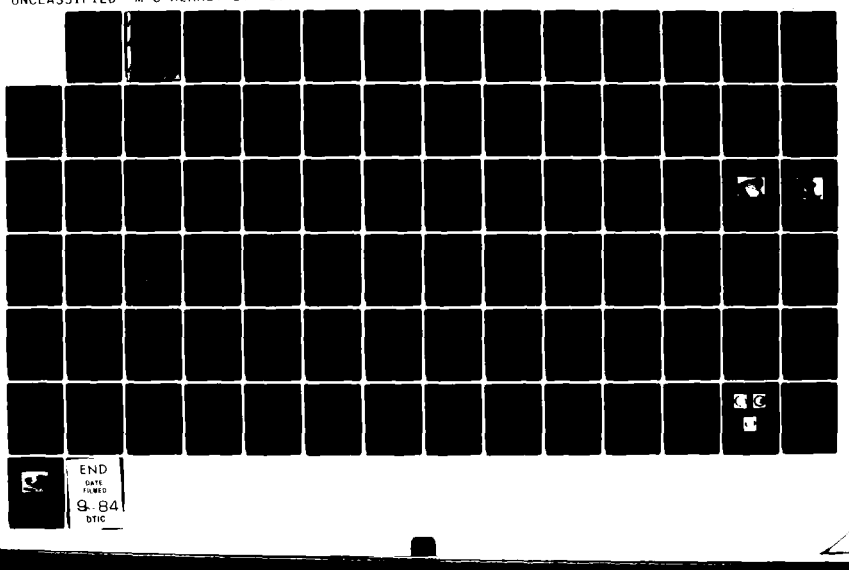

END
DATE FILMED
9-84
DTIC

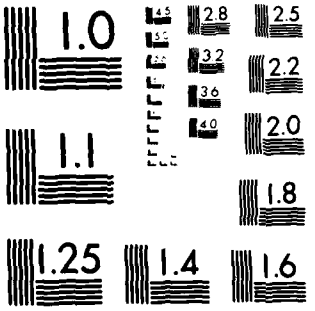

Research Report R84-2

FATIGUE OF SYNTHETIC FIBERS FOR MARINE ROPE APPLICATIONS

by
M.C. KENNEY
J.F. MANDELL
F.J. McGARRY

April 1984

MIT
DEPARTMENT OF MATERIALS SCIENCE AND ENGINEERING
SCHOOL OF ENGINEERING
MASSACHUSETTS INSTITUTE OF TECHNOLOGY
Cambridge, Massachusetts 02139

SECURITY CLASSIFICATION OF THIS PAGE *(When Data Entered)*

REPORT DOCUMENTATION PAGE		READ INSTRUCTIONS BEFORE COMPLETING FORM
1. REPORT NUMBER Research Report #R84-2	2. GOVT ACCESSION NO. AD-A144350	3. RECIPIENT'S CATALOG NUMBER
4. TITLE *(and Subtitle)* Fatigue of Synthetic Fibers for Marine Rope Applications		5. TYPE OF REPORT & PERIOD COVERED Final, April 1984 6. PERFORMING ORG. REPORT NUMBER
7. AUTHOR(s) M.C.Kenney F.J. McGarry J.F. Mandell		8. CONTRACT OR GRANT NUMBER(s)
9. PERFORMING ORGANIZATION NAME AND ADDRESS Department of Materials Science and Engineering School of Engineering, Mass. Inst. of Technology Cambridge, Massachusetts 02139		10. PROGRAM ELEMENT, PROJECT, TASK AREA & WORK UNIT NUMBERS
11. CONTROLLING OFFICE NAME AND ADDRESS Department of the Navy, Naval Sea Systems Command George Prentice 56W2 Washington, D.C. 20362		12. REPORT DATE April 1984 13. NUMBER OF PAGES 80
14. MONITORING AGENCY NAME & ADDRESS*(if different from Controlling Office)*		15. SECURITY CLASS. *(of this report)* unclassified 15a. DECLASSIFICATION/DOWNGRADING SCHEDULE
16. DISTRIBUTION STATEMENT *(of this Report)*		
17. DISTRIBUTION STATEMENT *(of the abstract entered in Block 20, if different from Report)*		
18. SUPPLEMENTARY NOTES		
19. KEY WORDS *(Continue on reverse side if necessary and identify by block number)* creep-rupture data for nylon 6,6 fatigue of synthetic fibers nylon rope, polyester, aramid		

20. ABSTRACT *(Continue on reverse side if necessary and identify by block number)*

S-N fatigue and creep-rupture data have been obtained for nylon 6,6 single fibers, interlaced yarns, and small ropes under a variety of loading conditions. The results show a similar degradation rate at each level of structure, with no apparant influence of interfiber effects. Cyclic lifetimes of single fibers of nylon 6,6 as well as polyester and aramid can be predicted from creep rupture models. Consistent with this model, the time failure is insensitive to frequency over a broad range. For each level of structure the strain at failure is the same whether tested in simple tension

DD FORM 1 JAN 73 1473 EDITION OF 1 NOV 65 IS OBSOLETE

S/N 0102-LF-014-6601

SECURITY CLASSIFICATION OF THIS PAGE *(When Data Entered)*

or under cyclic or creep loading. Failure modes were generally similar in creep rupture and cyclic fatigue tests; no effects of a slack load on each cycle was evident either in the failure mode or specimen lifetime.

INSTRUCTIONS FOR PREPARATION OF REPORT DOCUMENTATION PAGE

RESPONSIBILITY. The controlling DoD office will be responsible for completion of the Report Documentation Page, DD Form 1473, in all technical reports prepared by or for DoD organizations.

CLASSIFICATION. Since this Report Documentation Page, DD Form 1473, is used in preparing announcements, bibliographies, and data banks, it should be unclassified if possible. If a classification is required, identify the classified items on the page by the appropriate symbol.

COMPLETION GUIDE

General. Make Blocks 1, 4, 5, 6, 7, 11, 13, 15, and 16 agree with the corresponding information on the report cover. Leave Blocks 2 and 3 blank

Block 1. Report Number. Enter the unique alphanumeric report number shown on the cover.

Block 2. Government Accession No. Leave Blank. This space is for use by the Defense Documentation Center.

Block 3. Recipient's Catalog Number. Leave blank. This space is for the use of the report recipient to assist in future retrieval of the document.

Block 4. Title and Subtitle. Enter the title in all capital letters exactly as it appears on the publication. Titles should be unclassified whenever possible. Write out the English equivalent for Greek letters and mathematical symbols in the title (see "Abstracting Scientific and Technical Reports of Defense-sponsored RDT&E."AD-667 000). If the report has a subtitle, this subtitle should follow the main title, be separated by a comma or semicolon if appropriate, and be initially capitalized. If a publication has a title in a foreign language, translate the title into English and follow the English translation with the title in the original language. Make every effort to simplify the title before publication.

Block 5. Type of Report and Period Covered. Indicate here whether report is interim, final, etc., and, if applicable, inclusive dates of period covered, such as the life of a contract covered in a final contractor report.

Block 6. Performing Organization Report Number. Only numbers other than the official report number shown in Block 1, such as series numbers for in-house reports or a contractor grantee number assigned by him, will be placed in this space. If no such numbers are used, leave this space blank.

Block 7. Author(s). Include corresponding information from the report cover. Give the name(s) of the author(s) in conventional order (for example, John R. Doe or, if author prefers, J. Robert Doe). In addition, list the affiliation of an author if it differs from that of the performing organization.

Block 8. Contract or Grant Number(s). For a contractor or grantee report, enter the complete contract or grant number(s) under which the work reported was accomplished. Leave blank in in-house reports.

Block 9. Performing Organization Name and Address. For in-house reports enter the name and address, including office symbol, of the performing activity. For contractor or grantee reports enter the name and address of the contractor or grantee who prepared the report and identify the appropriate corporate division, school, laboratory, etc., of the author. List city, state, and ZIP Code.

Block 10. Program Element, Project, Task Area, and Work Unit Numbers. Enter here the number code from the applicable Department of Defense form, such as the DD Form 1498, "Research and Technology Work Unit Summary" or the DD Form 1634, "Research and Development Planning Summary," which identifies the program element, project, task area, and work unit or equivalent under which the work was authorized.

Block 11. Controlling Office Name and Address. Enter the full, official name and address, including office symbol, of the controlling office. (Equates to funding sponsoring agency. For definition see DoD Directive 5200.20, "Distribution Statements on Technical Documents.")

Block 12. Report Date. Enter here the day, month, and year or month and year as shown on the cover.

Block 13. Number of Pages. Enter the total number of pages.

Block 14. Monitoring Agency Name and Address (if different from Controlling Office). For use when the controlling or funding office does not directly administer a project, contract, or grant, but delegates the administrative responsibility to another organization.

Blocks 15 & 15a. Security Classification of the Report: Declassification/Downgrading Schedule of the Report. Enter in 15 the highest classification of the report. If appropriate, enter in 15a the declassification/downgrading schedule of the report, using the abbreviations for declassification/downgrading schedules listed in paragraph 4-207 of DoD 5200.1-R.

Block 16. Distribution Statement of the Report. Insert here the applicable distribution statement of the report from DoD Directive 5200.20, "Distribution Statements on Technical Documents."

Block 17. Distribution Statement (of the abstract entered in Block 20, if different from the distribution statement of the report). Insert here the applicable distribution statement of the abstract from DoD Directive 5200.20, "Distribution Statements on Technical Documents."

Block 18. Supplementary Notes. Enter information not included elsewhere but useful, such as: Prepared in cooperation with . . . Translation of (or by) . . . Presented at conference of . . . To be published in . . .

Block 19. Key Words. Select terms or short phrases that identify the principal subjects covered in the report, and are sufficiently specific and precise to be used as index entries for cataloging, conforming to standard terminology. The DoD "Thesaurus of Engineering and Scientific Terms" (TEST), AD-672 000, can be helpful.

Block 20. Abstract. The abstract should be a brief (not to exceed 200 words) factual summary of the most significant information contained in the report. If possible, the abstract of a classified report should be unclassified and the abstract to an unclassified report should consist of publicly- releasable information. If the report contains a significant bibliography or literature survey, mention it here. For information on preparing abstracts see "Abstracting Scientific and Technical Reports of Defense-Sponsored RDT&E," AD-667 000.

☆U.S. GOVERNMENT PRINTING OFFICE: 1980—703-100/7085 2-1

Research Report R84-2

FATIGUE OF SYNTHETIC FIBERS FOR MARINE ROPE APPLICATIONS

BY

M.C. Kenney
J.F. Mandell
and
F.J. McGarry

April 1984

Sponsored by
Naval Sea Systems Command Through the
MIT Sea Grant Program

Department of Materials Science and Engineering
School of Engineering
Massachusetts Institute of Technology
Cambridge, Massachusetts 02139

FOREWORD

This report contains the following two papers:

(1) Fatigue Behavior of Synthetic Fibers, Yarns, and Ropes

(2) The Effects of Sea Water and Concentrated Salt Solutions on the Fatigue of Nylon 6,6 Fibers.

Both of these papers derive from the PhD Thesis of Maryann C. Kenney titled "Effects of Fatigue and of Sea Water Environment on Nylon Fibers, Yarns, and Small Ropes" Department of Materials Science and Engineering, 1983.

The research is part of a broad study of the deterioration of synthetic marine rope. The overall study is headed by Prof. Stanley Backer of the Department of Mechanical Engineering; Mr. George Prentice is the Navy's technical liaison person on the project.

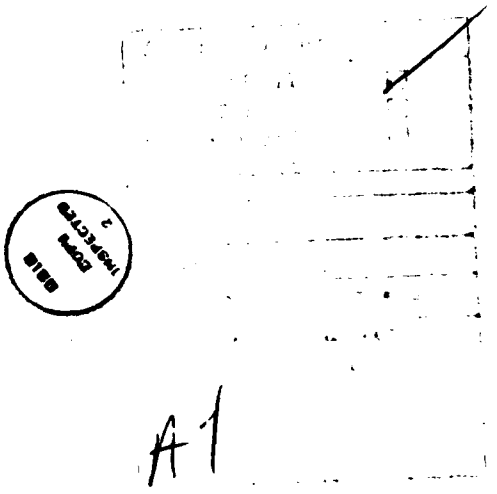

FATIGUE BEHAVIOR OF SYNTHETIC FIBERS, YARNS, AND ROPES

M. C. Kenney*, J. F. Mandell, F. J. McGarry

Department of Materials Science and Engineering
Massachusetts Institute of Technology
Cambridge, Mass. 02139 (USA)

SUMMARY

S-N fatigue and creep-rupture data have been obtained for nylon 6,6 single fibers, interlaced yarns, and small ropes under a variety of loading conditions. The results show a similar degradation rate at each level of structure, with no apparent influence of interfiber effects. Cyclic lifetimes of single fibers of nylon 6,6 as well as polyester and aramid can be predicted from a creep rupture model. Consistent with this model, the time to failure is insensitive to frequency over a broad range. For each level of structure the strain at failure is the same whether tested in simple tension or under cyclic or creep loading. Failure modes were generally similar in creep rupture and cyclic fatigue tests; no effect of a slack load on each cycle was evident either in the failure mode or specimen lifetime.

Submitted to Fibre Science and Technology

* Present address: Albany International Research Co., Dedham, Mass., 02026.

INTRODUCTION

Oriented fiber structures are used in many applications where a combination of good axial mechanical properties and light weight is required. The use of nylon fibers and yarns in marine ropes is one application which has grown considerably over the past 15 years. As with many applications, marine ropes in service are subjected to a complex history of static and cyclic mechanical loading [1] which may, in some cases, end in sudden and unexpected failure. This work is concerned with determining the mechanisms by which cyclic fatigue loading causes failure in oriented fiber structures, with emphasis on nylon single fiber and yarn properties, and additional work on small rope structures and other materials.

The effects of fatigue loading in polymers as a general class of materials is receiving increasing attention in the current literature (a recent review is given in ref. 2). In bulk polymers, failure during cycling can occur by a number of modes [3]. Some polymers such as nylon, with large hysteresis loops and poor thermal conductivity, may fail thermally as a result of internal hysteretic heating. The material may also respond to cycling as if a static load had been applied continuously for an equivalent period of time, with failures occurring at times and elongations similar to creep loading [4,5]. Finally, failure in bulk polymers may occur as a result of fatigue crack initiation and stable propagation, similar to that in metals. For nylon in fibrous form, some evidence exists for all three modes [6,7,8].

EXPERIMENTAL PROCEDURE

Fatigue testing was conducted using closed loop servohydraulic machines. Most tests were run in the load control mode, using a sine wave function. Ultimate tensile load was evaluated using a ramp test (constant loading rate) to failure at a rate equivalent to the averaged loading portion of the fatigue cycle. Fatigue testing was conducted to various percentages of this ultimate tensile load. The specimens were cycled between the maximum load and one-tenth of this value; i.e., the ratio $\sigma_{min}/\sigma_{max}$ (or stress ratio, R) was equal to 0.1. (Other R values have been used in some cases.) For single fiber fatigue testing, a specially designed steel beam support frame on pneumatic shock absorbers was constructed to minimize vibrations transmitted from the hydraulics and floor. A 2000-gram capacity load cell suspended from this frame registers approximately 1.5 gram noise. The number of cycles to failure was recorded for each specimen. Various parameters, such as load, displacement and hysteresis energy were monitored using a minicomputer.

A master frequency of 1 Hz was used for most testing, master frequency referring to the frequency corresponding to cycling at 100% of ultimate tensile load. The actual test frequency at each percentage of ultimate tensile load was then adjusted upward to maintain a constant average loading rate. Thus, the frequency was increased as the maximum load was decreased. Test frequency was kept as close as possible to this level, except where machine resonances required slightly lower values. The master frequency is given on each figure.

A cardboard tabbing system was used for testing of yarns and single fibers. A flexible silicone sealant was incorporated at the tab end to improve stress transfer, and protect the specimen from abrasion. Further into the tab the specimen was bonded with a rigid adhesive (Eastman 910). Using this tabbing method, the majority of fiber breaks occurred in the gage section, away from the grips, and were considered valid test results. For rope gripping, silicone and polyester adhesives were used to encapsulate rope ends into tapered metal fittings. The gage length between rigid adhesive points for single fibers and yarns was five inches (127 mm); the gage length between fittings for small ropes was four inches (102 mm).

Dead load creep rupture lifetimes for fibers and yarns were also measured using tabbed specimens. The top of the specimen was hung from a support and weights were suspended from the bottom. Selected creep rupture tests were also run on the servohydraulic machines to allow better monitoring of data; failure times in these tests agreed well with dead load data.

The primary material was DuPont 707 nylon 6,6 yarn, a standard rope yarn used commercially. The yarn consists of 210 lightly interlaced fibers producing a total of 1260 denier, taken from a single lot and merge; the single fiber diameter was 30 μm. The small rope was a 3/16 inch diameter double braided based on DuPont 707 nylon yarn, purchased from Sampson Ocean Systems. Except for single fiber creep rupture tests which were run at 65% RH, the humidity was not controlled. However, yarn creep rupture lifetimes obtained throughout the year were indistinguishable from those at 65% RH.

RESULTS AND DISCUSSION

Fiber, Yarn, and Small Rope Fatigue

Single fiber and yarn S-N data are plotted in Figure 1. The fatigue data are presented as normalized plots based on the single cycle ultimate tensile load for the conditions of that particular data set. Table 1 gives values of ultimate tensile load at failure for the specimens tested; these can be used to determine absolute load values for the S-N data. The lines on the graph show least square regressions of experimental data (not including single cycle ramp tests). Both sets of data are approximately linear, and show a steady decrease in lifetime with increasing maximum load. The linearity of this data and absence of a break in the curve imply that a single mechanism may operate throughout the fatigue range studied. These S-N curves are consistent with literature data [9,10,11]. For example, at about 60% of ultimate load, lifetimes are approximately 10^5 cycles.

It is important to note that the normalized graphs of the single fiber and yarn nearly superimpose. This can be seen from Figure 1, or by comparing the regression equations, with 95% confidence limits given in parentheses:

single fiber: $P/P_{ult} = 1.00\ (\pm .04) - .077\ (\pm .002)\ \log N$

yarn: $P/P_{ult} = 1.02\ (\pm .04) - .09\ (\pm .003)\ \log N$

where P is the load and N is cycles to failure. Thus, the two levels of structure show essentially the same fatigue resistance. This implies a common factor in the fatigue degradation of each, which does not appear sensitive to structural or interfiber effects at this level.

Fatigue data for the small ropes are also given in Figure 1. Tests were conducted at a frequency of 0.5 Hz. A fan was used to cool the rope during cycling to reduce the hysteretic temperature rise, which was otherwise substantial. Failure in the grips became a problem at lower loads and longer times. Grip failure points are indicated by arrows in Figure 1 and represent the lowest possible gage section lifetimes; gage section failure could have occurred at longer times. The rope data points fall close to those of both the single fiber and yarn. Even if a slight adjustment were made for differences in frequency, the points would fall at similar times, indicating that interfiber contact and other structural differences have a minimal effect in the small rope as well as in the yarn.

To further investigate possible interfiber or structural effects several studies were conducted, including interlaced and parallel yarn sections, added lubricants, and specimens composed of three contacting fibers. The DuPont 707 yarn is lightly interlaced by a jet of air blown orthoganally at the yarn during production, resulting in a lightly entangled point every two inches on the average, so all standard five inch yarn specimens probably contained at least one interlace. To investigate this effect, short sections of yarn (two inches) were prepared containing either an interlaced point or a completely parallel length. A standard fatigue S-N curve was determined for each (Figure 2). Fatigue data are identical for the parallel and interlaced specimens, as well as for specimens of standard length. Apparently, the interlace has

no significant effect on fatigue performance.

The effect of a lubricant on dry yarn performance was examined briefly using a silicone fiber finish, Union Carbide LE-9300, applied as an emulsion and catalyzed for full cure. A limited number of yarn fatigue tests at one load were conducted, and showed that the lubricant had no significant effect on the cycles to failure. A few tests were also run after the application of a standard silicone lubricating spray, and again no effect was found. This is not surprising in view of the absence of interfiber effects already demonstrated.

In a final study of interfiber effects, specimens were prepared with three fibers twisted together (two turns per inch). Fatigue data for these are compared to normalized single fiber lifetimes in Figure 3. Lifetimes for specimens with three fibers in contact are clearly comparable to those for single fibers at this low twist level.

All of the data reported in this section indicate that the single fiber fatigue behavior determines the yarn and, apparently, small rope fatigue behavior without any significant complications. While the average single fiber tensile strength is not completely realized in the average yarn strength, due to long recognized statistical bundle effects [12], the rate of loss of the initial tensile strength in fatigue (slope of the normalized S-N curve) is similar for all three structures. Interlace regions and added lubricants do not affect yarn fatigue. However, in highly twisted yarns and in larger rope structures with more lateral pressure and relative movement,

interfiber interactions and lubricant performance could become important.

Frequency Effects

As interfiber effects at the yarn level have no significant effect on fatigue performance under the conditions studied, the controlling mechanism must, therefore, be the individual response of the fibers to the applied loading. The failure mode under the applied loading may be dominated either by creep rupture (depending on time under load), traditional fatigue crack initiation and growth (depending on the number of cycles [3]), or hysteretic heating and the associated temperature rise. The dominance of a particular effect may be determined by varying the fatigue loading parameters and frequency.

Figure 4 gives fatigue data for single fibers tested at frequencies of 0.1, 1.0, and 6.2 Hz. The 0.1 and 1.0 Hz tests were conducted in the usual manner with the frequency adjusted upward to maintain constant loading rate. The 6.2 Hz tests, however, could not be adjusted upward because of machine resonances, and were run at a constant frequency; this should have little effect over this broad range of frequencies. Note that the data are plotted as a function of log time to fail, rather than cycles to fail. The total test lifetime is equivalent regardless of test frequency, and is also similar to constant force, creep rupture data also shown in Figure 4. These data indicate that single fibers fail according to a total time under load criterion.

Corresponding fatigue data for yarns tested at frequencies of 0.1, 1.0 and 10 Hz are given in Figure 5. (Again, adjustment could not be made exactly for the 10 Hz tests because of machine resonance and performance limits.) Temperature change from hysteretic heating was monitored for the highest test frequency using a temperature sensitive lacquer (Omega Lac 100). No color change was observed in the lacquer, indicating that the temperature did not exceed 100°F. This is consistent with the literature [7] and shows that complications of a thermal failure mode are not present. An intensive series of tests was also run on yarns at these frequencies at two specific load levels (80% and 60% of the 1 Hz ramp strength). Specimens were prepared identically and tested in random order. Time and cycles to fail for these individual specimens are given in Table 2. Both sets of data show that yarns follow a time under load criterion, as do the single fibers. Within the range of experimental scatter, the time to fail is constant regardless of the frequency of testing over the three frequencies used in this study (0.1, 1.0, 10 Hz). The common time under load failure dependence of both fibers and yarns is consistent with the equivalent S-N behavior observed at 1 Hz. This type of frequency dependence contrasts with that found in the literature for bulk nylon where crack growth rate per cycle, rather than total test time, remains similar as frequency is changed [3]. The observed contrast in behavior may result either from the dimensional characteristics or oriented structure of the fibers, or from material differences. Studies on acrylic and

nylon fibers [6,13] have shown decreasing time to fail with increasing frequency, but the extremely high frequencies used (50 - 90 Hz) could have affected these results.

Failure Strain

Table 3 gives failure strains for single fibers, yarns, and small ropes for various types of loading. Under all loading conditions studied (fatigue, creep, and single cycle ramp tests) the total cumulative strain reached at failure is roughly constant for a given level of structure. The overall strain reached is, of course, influenced by the structure; it increases from fiber to rope as the structure becomes more geometrically complex. Similar failure strains are also reached regardless of test frequency, as is shown for yarns in Table 2. Figure 6 shows that the strain accumulating with total test time is remarkably insensitive to the frequency or number of cycles. Just prior to failure the strain increases rapidly as some fibers fail. Tests with a combination of loading conditions, as in tests where cycling is following by ramp testing, also show a constant cumulative failure strain equivalent to the initial ramp value.

The observation that failure occurs at a particular strain for any level of structure, for all loading conditions, provides further strong support for the dominance of simple creep rupture in controlling failure. The creep behavior of the single fiber, as moderated by increasing structural complexity, may determine the limiting extension in each level of structure studied. Within the single fiber, on a molecular level, this

could be interpreted from various nylon models as either the accumulation of a critical number of taut tie molecules in the amorphous region [14], or as reaching a limited extension of the oriented interfibrillar regions [15].

Fractographic Study

Two types of fracture surfaces were observed in this study which are generally similar to those reported in the literature [6]. Figure 7 shows the most typical surface, the classic scallop shell transverse fracture observed in many textile fibers. In this fracture, a crack initiates at the surface, then grows generally transverse to the fiber axis through a slow growth region. Finally, there is a fairly sharp transition to the fast fracture region. Figure 8 shows a second type of fracture which also appears to initiate at the surface, but then is dominated by splitting generally parallel to the fiber axis, in a mode described as fibrillated [6].

Transverse failures were observed for all fatigue breaks at high loads and for most fatigue breaks at low loads. In approximately five percent of breaks at low loads in yarns a fibrillated fracture was observed. This behavior is not unique to fatigue breaks, as both types of fractures were also observed for specimens from creep rupture tests at similar loads. This finding is contrary to reports in the literature [6] that in similar fibers the axial cracking mode is indicative of a unique fatigue failure mode and requires a slack load condition, which has been suggested to reduce fatigue lifetimes. The origin of this difference could be the higher

frequency (50 Hz) used in the ref. 6 tests, which could not be duplicated here.

Several fatigue tests were conducted on yarns using a slack loading condition (R = 0) at 1 Hz. The data shown in Figure 9 fall within the previously determined fatigue lifetime scatter. Apparently, a period of slack load has no effect on yarn fatigue behavior under these conditions, compared with tests at the usual R = 0.1.

Slack load fatigue tests were also run on single fibers, but at a frequency of 20 Hz. Because of dynamic (recording) effects, the measured load peak values were adjusted downward by 10% to give a better estimate of the actual loading. The adjusted data are plotted in Figure 10, along with the fatigue data at 1 Hz. Two features are apparent: the high frequency data follow quite closely the fatigue behavior at 1 Hz, and the presence of a slack load does not reduce the fatigue lifetime below the expected range. Fiber fracture surfaces from these tests also show a mixture of transverse and axial types. Our data, including observation of the axial mode in creep as well as cyclic tests, suggest that the axial splits do not require cyclic or slack loads, and that the mode of cracking does not influence the lifetime over the frequency range studied here. The occurrence of axial cracking clearly reflects the longitudinal structure of nylon with some preferred path between fibril or microfibril units. Kevlar fibers, with a more nearly perfect orientation, were observed to fail in the axial mode under all loading conditions in this study.

Failures of the type described here suggest a fatigue crack growth controlled failure. In bulk polymers this would usually suggest a cyclic, rather than creep, dominated behavior which could be considered in a fracture mechanics context. However, previous results for the strains at failure, and the similar times to fail under differing conditions are more consistent with a creep rupture mode. While cracks are clearly associated with eventual failure of the fibers, they may not represent the typical fatigue cracks which dominate bulk polymer breakdown [3], but rather represent a limiting rearrangement and extension of the fiber structure which is a consequence of creep.

Residual Strength

Residual strength tests were conducted at various fractions of specimen lifetimes, typically 25, 50, and 75% of the mean lifetime, at a variety of load levels. Residual strength was determined within approximately one minute of the end of cycling. The single fiber data in Figure 11 show that the residual strength is almost equal to the original ultimate strength under all conditions. Thus, failure must occur in a sudden death fashion, with little decrease in strength before the fiber fails. The residual strain to failure shows a more gradual decrease as creep occurs. For a single fiber tested at 80% of the UTS for 75% of its lifetime, the residual strain to failure is approximately 75% of the initial value.

Higher levels of structure show somewhat more gradual

property changes due to structural rearrangements and single fiber failures. For example, a yarn tested at 70% of its UTS contained almost exactly 70% of the original fibers unbroken just prior to failure. Thus, strength degradation in yarns and small ropes may be explained more by accumulating broken fibers than by changes in unbroken fibers. Permanent strains accumulating during fatigue are also greater with yarns and ropes. A small rope tested at 60% of its UTS for 75% of its lifetime has a permanent creep strain of approximately 60% of its original failure strain.

Creep Rupture Model for Fatigue Life

Evidence for a simple creep rupture mechanism controlling failure in single fibers, yarns and small ropes appears quite strong. Normalized S-N curves are similar for all three structures. Interfiber effects are minimal in these yarns and small ropes, and do not appear to influence failure. Time to fail at the same load remains constant over a range of frequencies for both single fibers and yarns. Also, a constant strain is reached at failure, for a given structure, regardless of loading pattern or frequency. All of these results point strongly to a simple creep rupture mechanism. The constant failure strain [16] and time to failure regardless of frequency [17] have been reported in earlier fiber studies under more restrictive loading conditions.

A creep rupture failure mechanism may be analyzed using the concepts of reaction rate theory and accumulation of damage [5]. This approach has been applied in the literature to both fibers and bulk materials [4,5]. According to one typical approach [4], failure is approximated by dividing the sinusoidal fatigue wave into many small increments and weighting each increment by its failure time under pure creep loading; when the fractional lifetimes sum to 1, failure occurs. (This criterion is analogous to Miner's rule used in cycle dominated cases.) Failure then may be expressed as:

$$\int_0^{t_b} \frac{d(t)}{\tau_b\ \sigma(t)} = 1 \qquad (1)$$

where τ_b is the time to fail under constant stress (creep rupture), σ is the applied stress, and t_b is the time to fail under sinusoidal stress.

Creep rupture is expressed in the form:

$$\tau_b \approx A \exp^{-B\sigma} \qquad (2)$$

where A and B are experimentally measured constants. The creep rupture data which have been collected for single fibers, yarns, and small ropes all follow this type of relationship. For the case of sinusoidally varying load, the appropriate expression for σ is:

$$\sigma\ (t) = P + Q \sin\ (\omega t) \qquad (3)$$

When these expressions are substituted into Eq. (1) the integral

may be solved using a zero order modified Bessel function giving the time to break as:

$$t_b = \frac{\hat{t}(p)}{I_o(BQ)} \qquad (4)$$

where $\hat{t}(p)$ is the time to fail under a constant load equal to the mean load p, B is the slope from Eq. (2), and Q is the amplitude from Eq. (3). To summarize, creep rupture times are integrated over a varying load to calculate the fatigue failure time.

Calculated failure times based on yarn and fiber creep rupture data are compared to the actual experimental fatigue data points in Figures 12 and 13. (Confidence limits on the graphs were determined by finding the 95% limits on the creep rupture pre-exponential terms, and then using these bounds for the creep rupture equation in the integration procedure.) Single fiber behavior is very well predicted by the creep rupture model. This behavior is common to several other highly oriented fibers which were also examined briefly. Aramid (Kevlar 49) and polyester (DuPont D608 PET) single fiber data, shown in Figures 14 and 15, both conform to the model.

In contrast, yarn (Figure 12) does not conform as well; the data consistently fall below the model prediction. Note that different sets of creep rupture data are used in the single fiber and yarn predictions; single fiber creep is used in the single fiber prediction and yarn creep is used in the yarn prediction. Since it has been shown that the single fibers and yarns have the same normalized S-N behavior under cyclic loading at different frequencies, it is clear that the

difference in model accuracy between yarns and single fibers must derive from differences in their creep rupture behavior. Figure 16 compares the creep rupture curves for single fibers and yarns. (The ultimate load used to normalize the creep data is determined in a ramp test with a total failure time of approximately 0.5 seconds). The yarn creep rupture curve is clearly less steep. A comparison of Figures 12 and 13 shows that the yarn cyclic fatigue data are predictable from the creep rupture model if the single fiber creep rupture curve is used in the prediction.

The less steep creep rupture slope of the yarn may be explained by the observation that, in a yarn structure under constant dead load, individual broken fibers may be caught within the structure and reloaded along part of their length. In a yarn undergoing cycling, on the other hand, the structure continually opens and closes, allowing broken fibers to work free and become completely unloaded; this is, in fact, visually observed.

The question of relative fiber movement within the yarn during cycling was examined in a series of yarn fatigues at varying R ratios (0.1, 0.5, and 0.8). Figure 17 indicates that higher R ratios, resulting in reduced opening and closing of the structure, approach the limit of constant loading or creep rupture at R = 1.

A series of experiments was conducted to directly observe the behavior of yarns containing some cut fibers to simulate broken fibers. In these experiments, several fibers within the structure were cut, their ends and starting positions

marked, and displacement of the ends examined after 1000 cycles at 70% of ultimate load. From the location of the fiber ends, the amount of strain on the cut fibers, compared to the yarn as a whole, may be calculated. The results given in Table 4 show an increasing amount of average strain over the cut fiber length, and corresponding greater average loading in the cut fibers at higher R ratios, approaching a maximum during creep rupture. Thus, the fibers are only partially unloaded, and the less steep creep rupture curve of yarn may derive from this effect. Cycling at the usual R = 0.1 reduces this process, so the fiber and yarn data agree in cyclic fatigue. Similar reloadings may occur in small ropes as well, although the amount will necessarily be affected by the complex geometric structure.

CONCLUSIONS

The fatigue resistance of nylon single fibers, yarns and small ropes are all nearly identical on normalized S-N scales, at all frequencies tested. Yarns and single fibers fail by a creep rupture mode depending on the total time under load, not the number of cycles. A cumulative time under load, creep rupture model for fibers can accurately predict the failure in cyclic tests at different frequencies. Other oriented fibers (polyester and aramid) also agree with this creep rupture model. Consistent with a creep rupture dominated mode, the strain at failure for a given structure is independent of the type of loading, including ramp (tensile test), creep rupture, or cyclic fatigue. The model is less accurate for yarns, as

the baseline creep rupture curves become less steep in going from fiber to yarn. This may arise from broken fibers which are partially reloaded in the higher levels of structure. However, the yarn cyclic data are accurately predicted when the single fiber creep rupture data are used in the model prediction.

ACKNOWLEDGEMENT

This research is part of a broad study of the deterioration of synthetic marine rope supported by the Naval Sea Systems Command through the MIT Sea Grant Program. Mr. George Prentice is the Navy's technical liaison person on the project.

REFERENCES

1. N. Starsmore, M.G. Halliday and W.A. Ewere, Proc. Int. Symp. Ocean Engr.-Ship Handling, Gothenberg, Sweden (1980), paper 13.

2. R.W. Hertzberg, J.A. Manson, "Fatigue of Engineering Plastics", (Academic Press, New York 1980).

3. J.A. Manson, R.W. Hertzberg, CRC Critical Reviews in Macromolecular Science 1 (1973) 433.

4. G.B. McKenna, R.W. Penn, Polymer 21 (1980) 213.

5. B.D. Coleman, J. Poly. Sci. 20 (1956) 447.

6. A.R. Bunsell, J.W.S. Hearle, J. App. Poly. Sci. 18 (1974) 267.

7. R.L. Hamilton, C.H. Miller Jr., Text. Res. J. 34 (1964) 20.

8. J.W.S. Hearle, J. Mat. Sci. 2, (1967) 474.

9. I. Narisawa, M. Ishikawa, H. Ogawa, J. Poly. Sci. 15 (1977) 1055.

10. A.R. Bunsell, J.W.S. Hearle, J. App. Poly. Sci. 18 (1974) 267.

11. W.T. Kelley, Text. Res. J. 35 (1965) 852.

12. M.M. Platt, W.G. Klein, W.J. Hamburger, ibid 22 (1952) 641.

13. W.J. Lyons, ibid 32 (1962) 553.

14. A. Peterlin, J. Poly. Sci. A-2, 7 (1969) 1151.

15. D.C. Prevorsek, P.J. Harget, R.K. Sharma, A.C. Reimschuessel, J. Macromolec. Sci. - Phys. B8, 1-2 (1973) 127.

16. J.W.S. Hearle, E.A. Vaughn, Rheol. Acta 9 (1970).

17. A.R. Bunsell, J.W.S. Hearle, Rheol. Acta 13 (1974) 711.

Table 1

ULTIMATE LOAD AND ELONGATION IN

SINGLE CYCLE RAMP TESTS

	Ultimate*		
	Load	Stress (MPa)	Elongation (%)
FIBER	68.1 gm (± 2.0)	965	15.0 (± .75)
YARN	11.61 kg (± .43)	779	17.0 (± 1.4)
ROPE	605 kg (± 21)	---	40.9 (± 2.0)

* approximate failure time = 0.5 sec.

Table 2

FATIGUE LIFETIME OF

YARN AT VARIOUS FREQUENCIES

(single specimen data)

Frequency (Hz)	Log (Cycles to Fail)	Log (Time to Fail, sec)	Total Elongation (%)
80% Ultimate Load*			
0.167	1.690	2.467	16.7
	1.716	2.493	16.3
1.67	2.846	2.624	>16.3
	2.723	2.501	17.8
10	3.223	2.223	16.3
	3.625	2.625	18.7
60% Ultimate Load*			
0.167	3.897	4.674	17.1
	3.312	4.089	18.4
	4.152	4.930	15.4
	3.685	4.462	17.5
1.67	4.983	4.760	17.4
	4.527	4.305	17.5
	4.522	4.300	17.6
10	5.868	4.868	17.6
	5.810	4.810	--
	5.649	4.649	17.5
	5.549	4.549	17.0

*as measured in a 1 Hz test

Table 3

COMPARISON OF SINGLE CYCLE RAMP,

FATIGUE, AND CREEP VALUES OF FAILURE STRAIN

	Failure Strain (%)		
	Ramp	Fatigue*	Creep*
FIBER	15.0 (± .75)	14.6	14.4
YARN	17.0 (± 1.4)	18.9	18.9
ROPE	40.9 (± 2.0)	41.9	41.4

*Single specimen at 70% ultimate load, typical data.

Table 4

ANALYSIS OF FIBER MOVEMENT IN YARN AFTER 1000 CYCLES

AT 70% ULTIMATE LOAD, 1 Hz

R Ratio	Number of Cut Fibers	Average % Strain Along Cut Fiber Length
0.1	9	0
0.5	3	1.5
	6	0
0.8	4	5.4
	6	3.1
1.0	5	7.9
	5	4.7

Figure Captions

Fig.	Caption
1.	S-N Fatigue Data for DuPont 707 Nylon Single Fibers, Yarns, and 3/16 in. Double Braided Rope.
2.	S-N Fatigue Data for Parallel and Interlaced Sections of Nylon Yarn.
3.	S-N Fatigue Data for Single Nylon Fibers and for Three Fibers in Contact.
4.	Fatigue Data for Single Nylon Fibers at Several Frequencies, Plotted vs. Total Test Time For Comparison with Creep Rupture Data
5.	Fatigue Data for Nylon Yarns at Several Frequencies Compared with Creep Rupture Data.
6.	Elongation During Fatigue for Nylon Yarns at Three Frequencies, Tested at 60% of Ultimate Load.
7.	Fracture Surface of Nylon Fiber Failed in Fatigue at 90% of Ultimate Load.
8.	Fracture Surface of Fiber From Nylon Yarn Failed in Fatigue at 50% of Ultimate Load.
9.	Effect of Slack Condition During Each Cycle in Fatigue of Nylon Yarns.
10.	Effect of Slack Condition at High Frequency on Single Nylon Fibers.
11.	Residual Strength of Single Nylon Fibers After Fatiguing Various Fractions of Their Lifetimes at Three Load Levels.
12.	Comparison of Single Nylon Fiber Cyclic Fatigue Data with Prediction From Creep Rupture Based Model.
13.	Comparison of Nylon Yarn Cyclic Fatigue Data with Prediction.
14.	Comparison of Single Aramid Fiber Cyclic Fatigue Data with Prediction.
15.	Comparison of Single Polyester Fiber Cyclic Fatigue Data with Prediction.

Fig.	Caption
16.	Comparison of Creep Rupture Data for Nylon Single Fibers, Yarns and 3/16 in. Double Braided Rope.
17.	Effect of R Ratio on Fatigue of Nylon Yarns.

Figure 1

FATIGUE LIFETIMES
DuPONT 707 NYLON SINGLE FIBER, YARN,
AND 3/16" DOUBLE BRAIDED ROPE

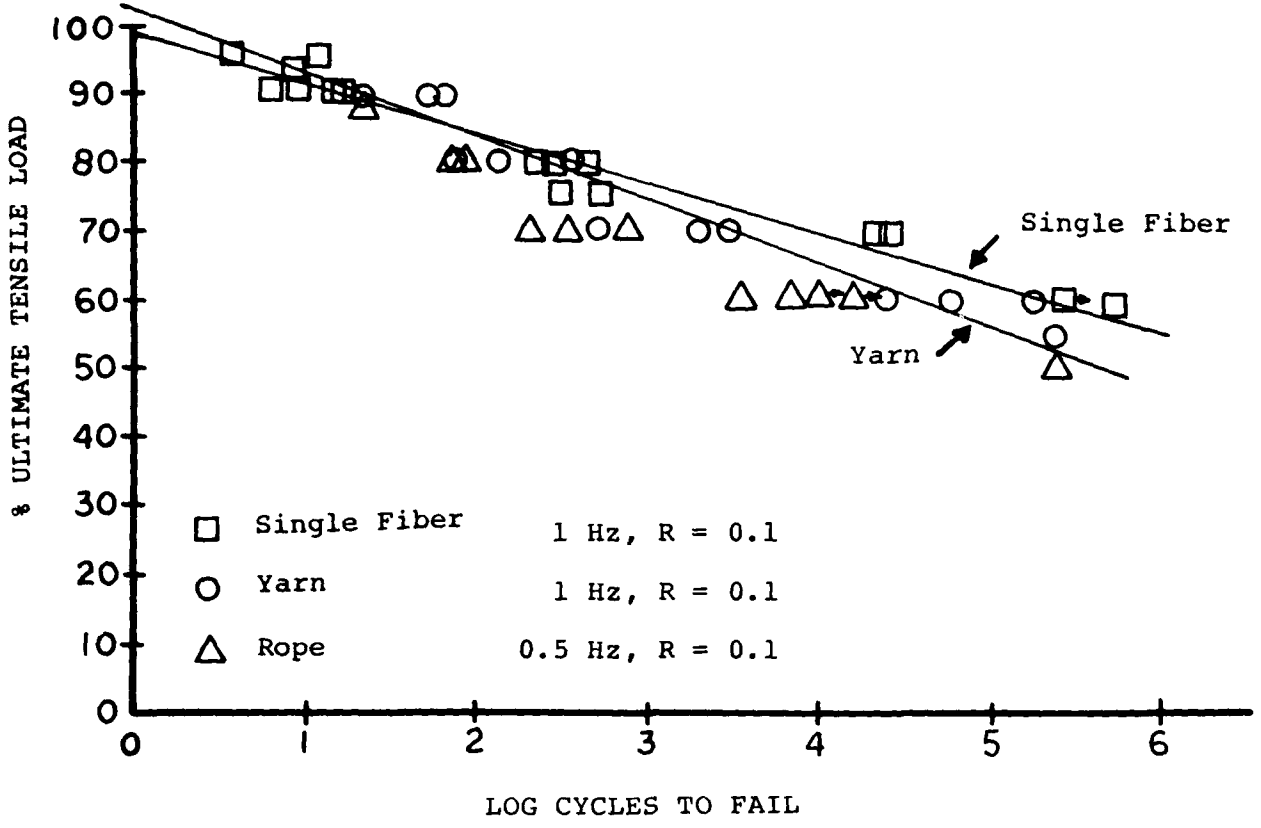

Figure 2

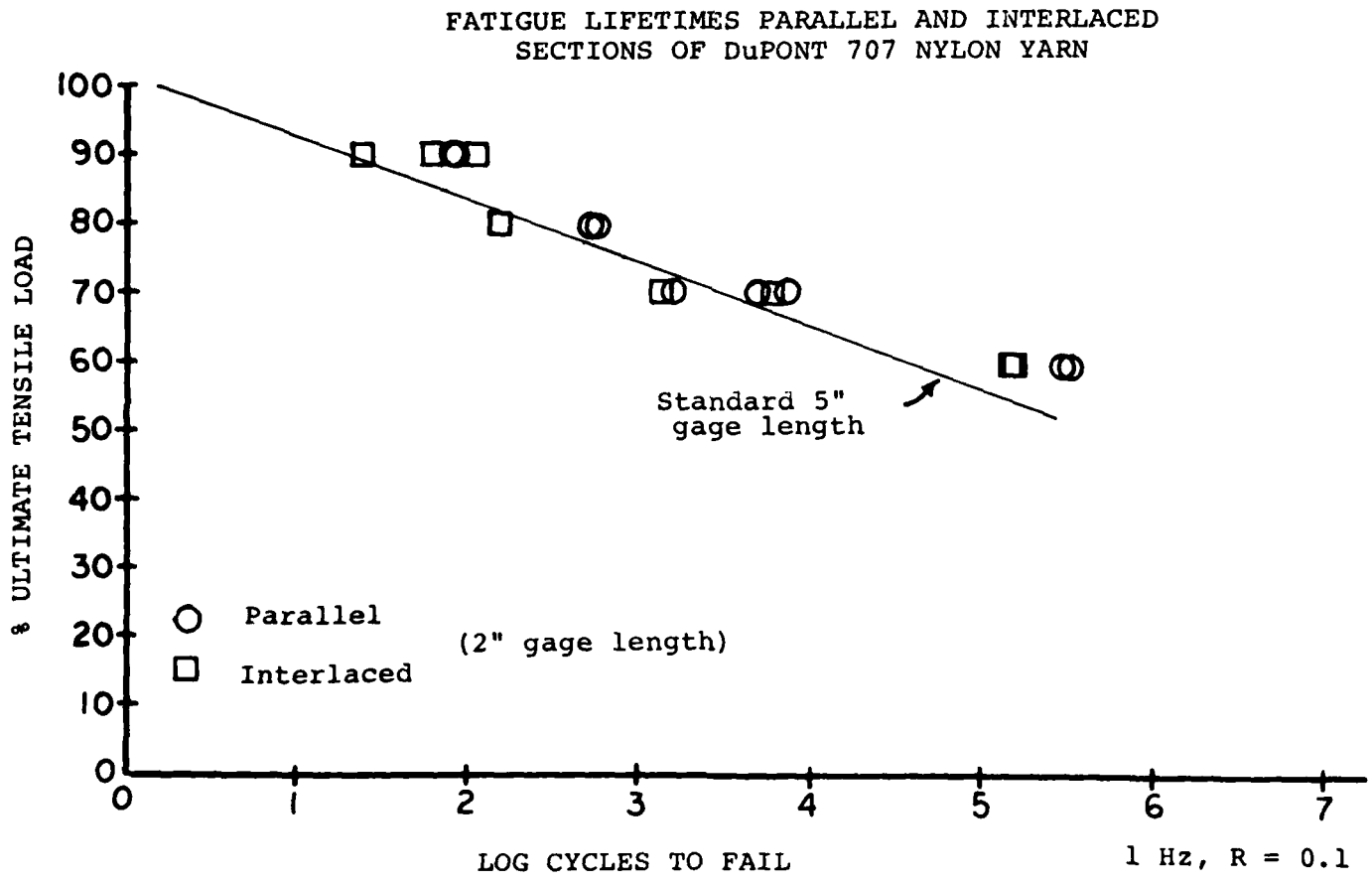
FATIGUE LIFETIMES PARALLEL AND INTERLACED
SECTIONS OF DuPONT 707 NYLON YARN
% ULTIMATE TENSILE LOAD
100
90
80
70
60
50
40
30
20
10
0
0
1
2
3
4
5
6
7
Standard 5"
gage length
Parallel
Interlaced
(2" gage length)
LOG CYCLES TO FAIL
1 Hz, R = 0.1

Figure 3

FATIGUE LIFETIMES
DuPONT 707 SINGLE FIBER IN AIR
(1 fiber, and 3 fibers in contact)

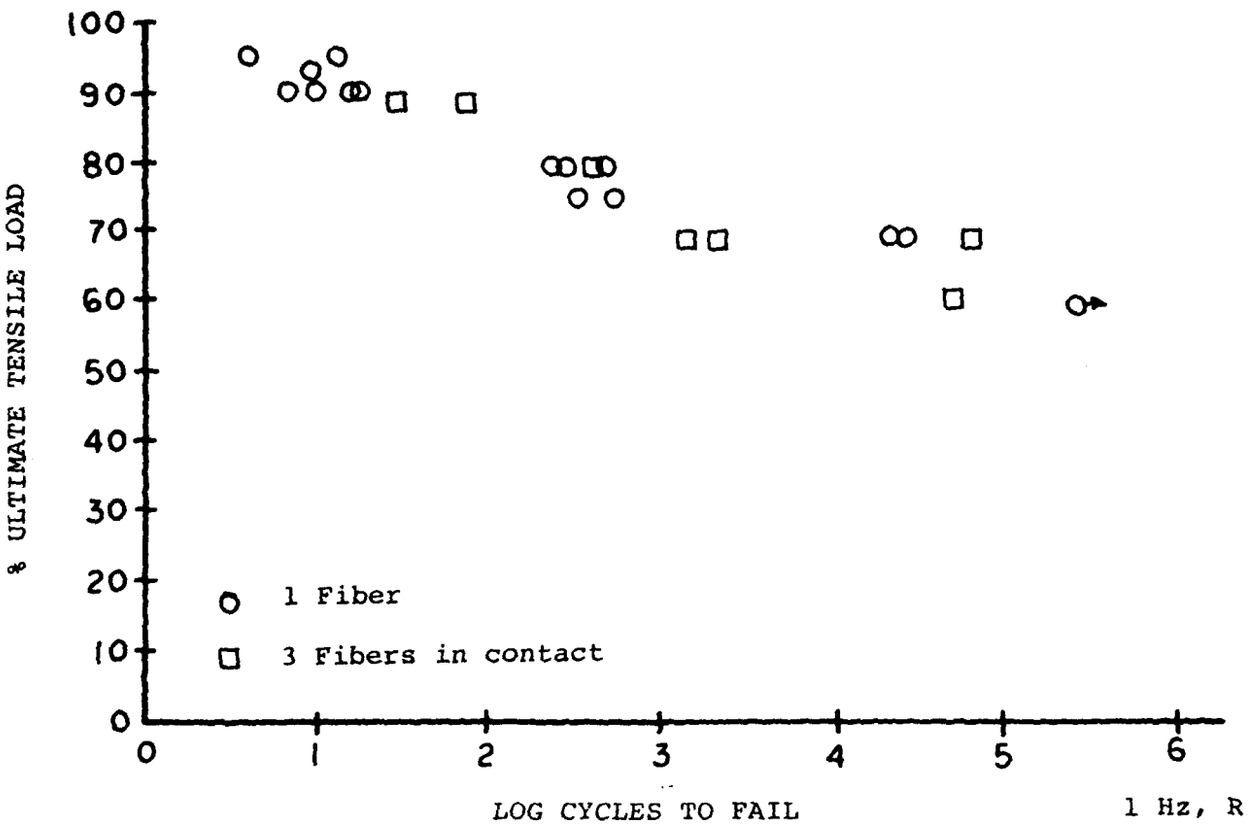

1 Hz, R = 0.1

Figure 4

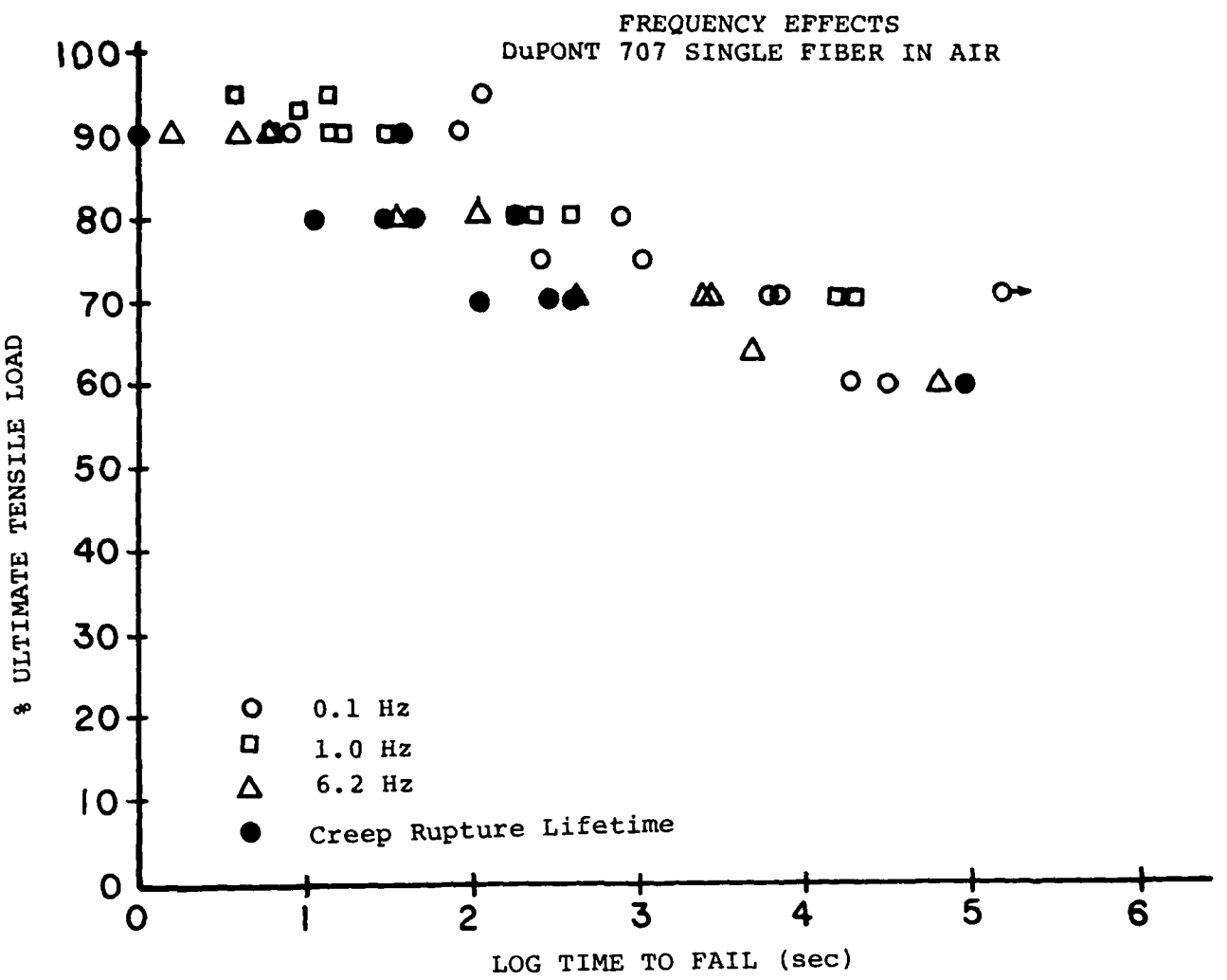
FREQUENCY EFFECTS
DuPONT 707 SINGLE FIBER IN AIR
% ULTIMATE TENSILE LOAD
100
90
80
70
60
50
40
30
20
10
0
0.1 Hz
1.0 Hz
6.2 Hz
Creep Rupture Lifetime
0
1
2
3
4
5
6
LOG TIME TO FAIL (sec)

Figure 5

FREQUENCY EFFECTS
DuPONT 707 NYLON YARN IN AIR

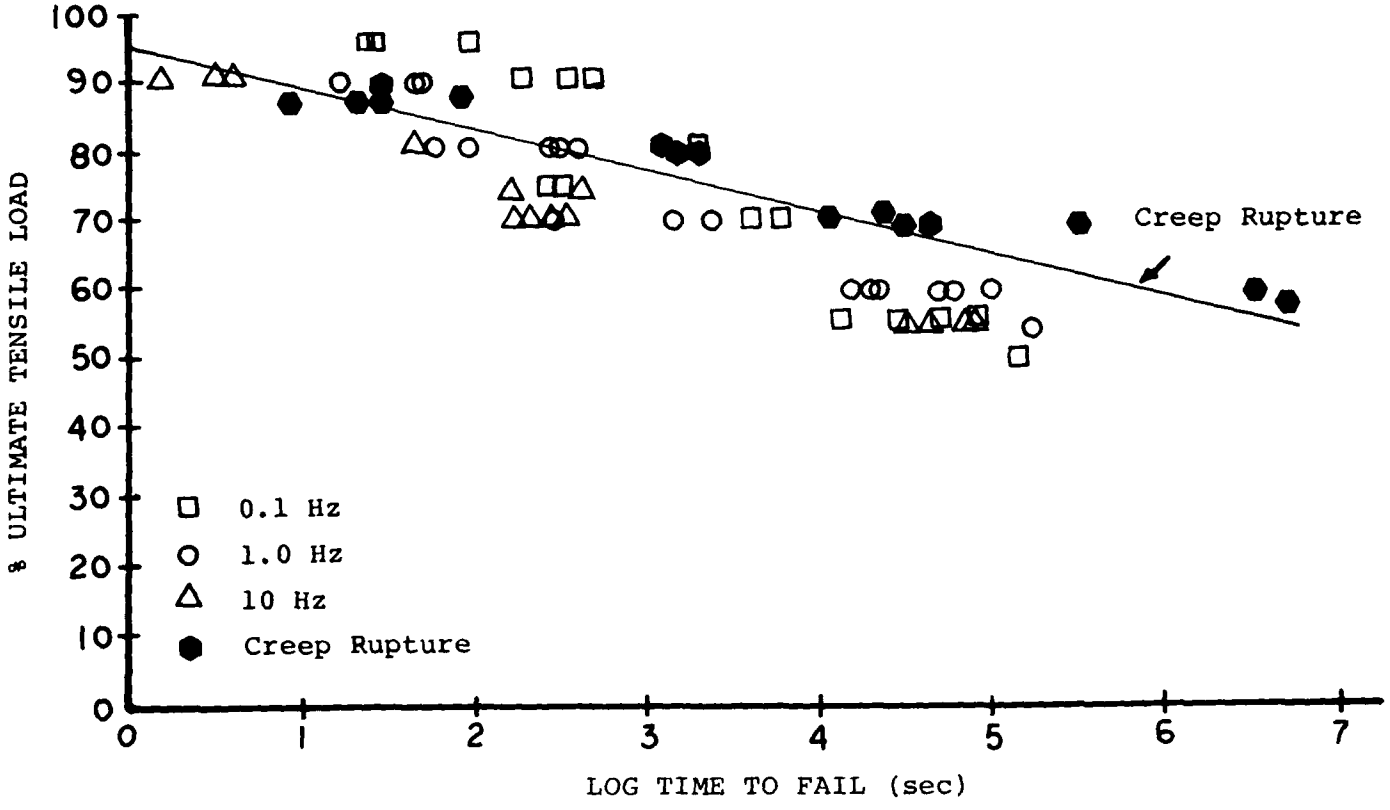

Figure 6

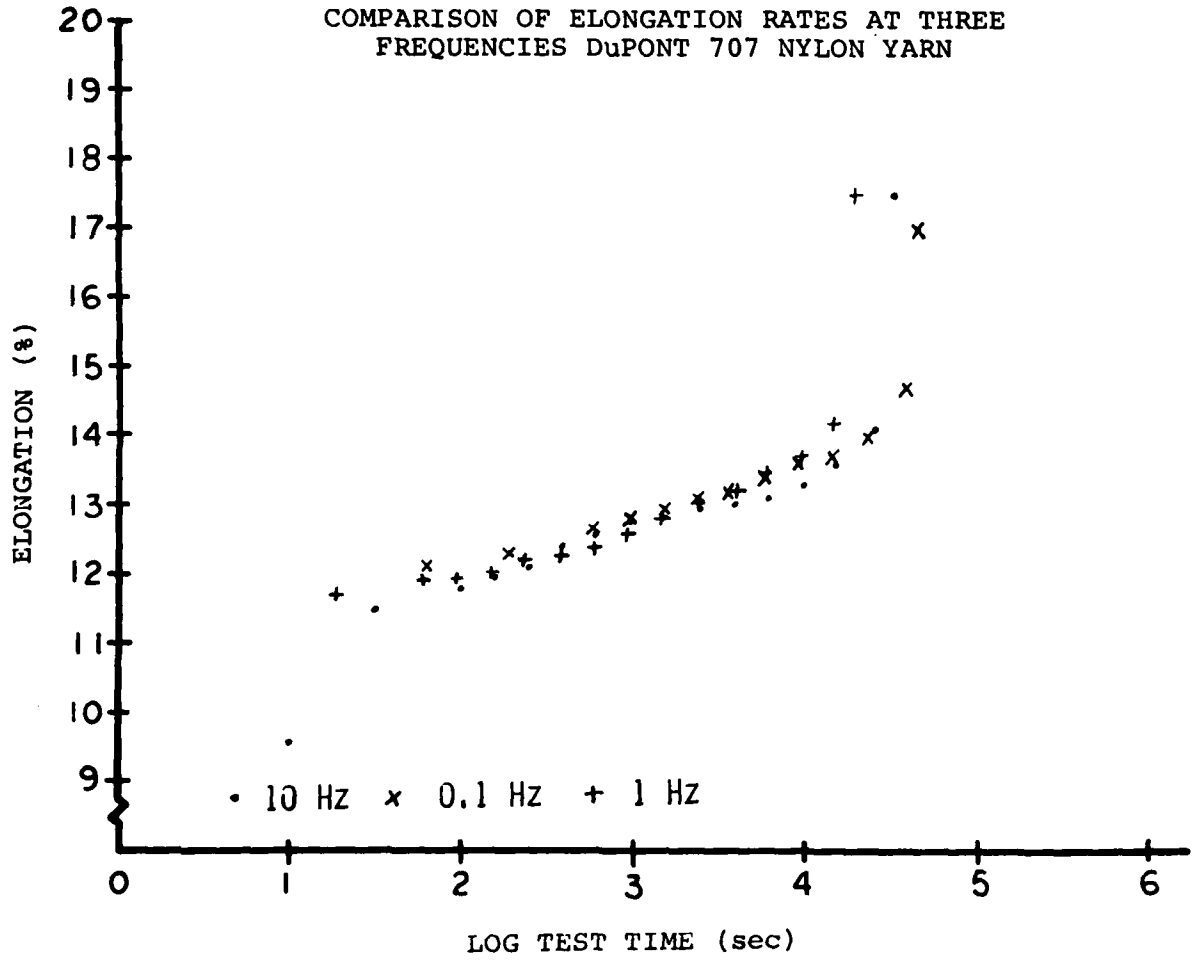
COMPARISON OF ELONGATION RATES AT THREE FREQUENCIES DuPONT 707 NYLON YARN
ELONGATION (%)
20
19
18
17
16
15
14
13
12
11
10
9
• 10 Hz × 0.1 Hz + 1 Hz
0
1
2
3
4
5
6
LOG TEST TIME (sec)

FATIGUE FRACTURE SURFACE OF SINGLE DRY
FIBER CYCLED AT 90% OF THE ULTIMATE LOAD

Figure 7

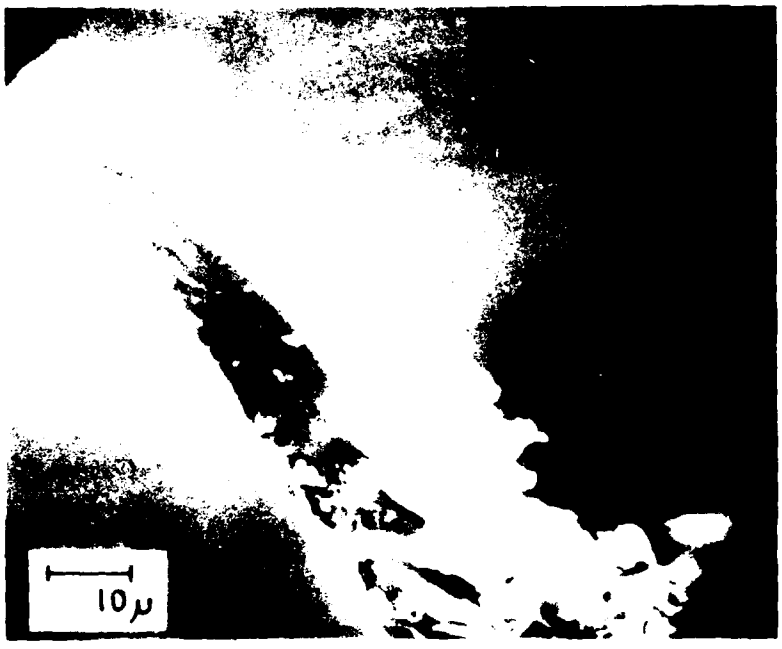

Figure 8

FATIGUE FRACTURE SURFACE OF FIBER FROM A DRY YARN CYCLED AT 50% OF THE ULTIMATE LOAD

Figure 9

EFFECT OF SLACK LOADING ON FATIGUE LIFETIMES OF DuPONT 707 NYLON YARN

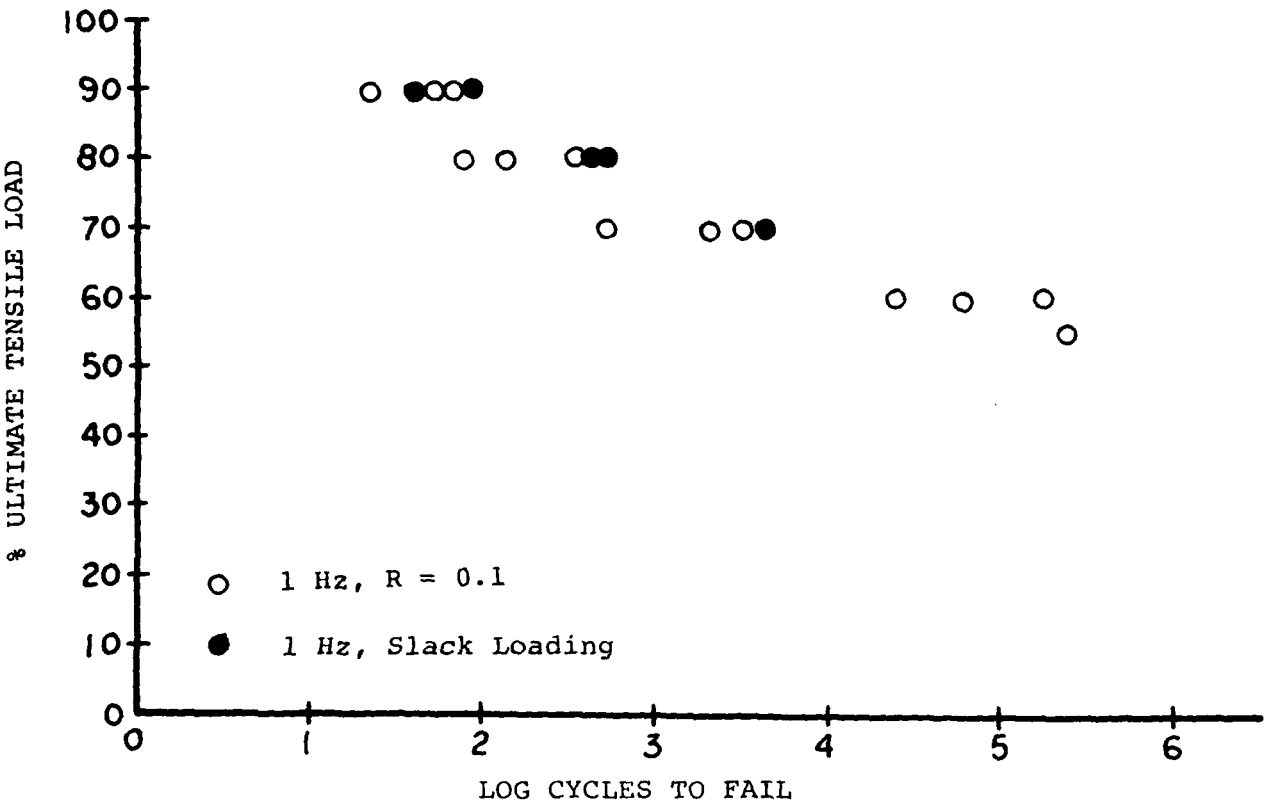

Figure 10

EFFECT OF HIGH FREQUENCY SLACK LOADING ON
FATIGUE LIFETIMES OF DuPONT 707 SINGLE FIBER

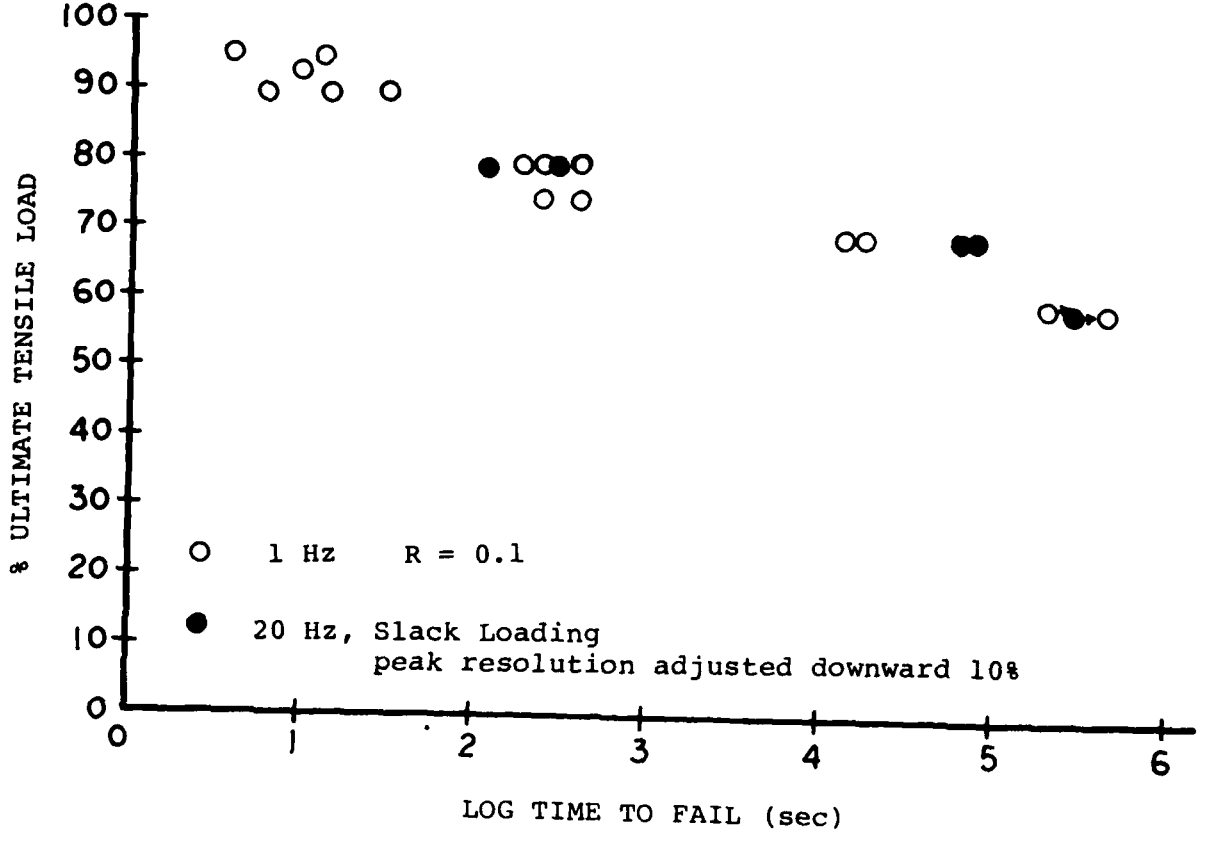

Figure 11

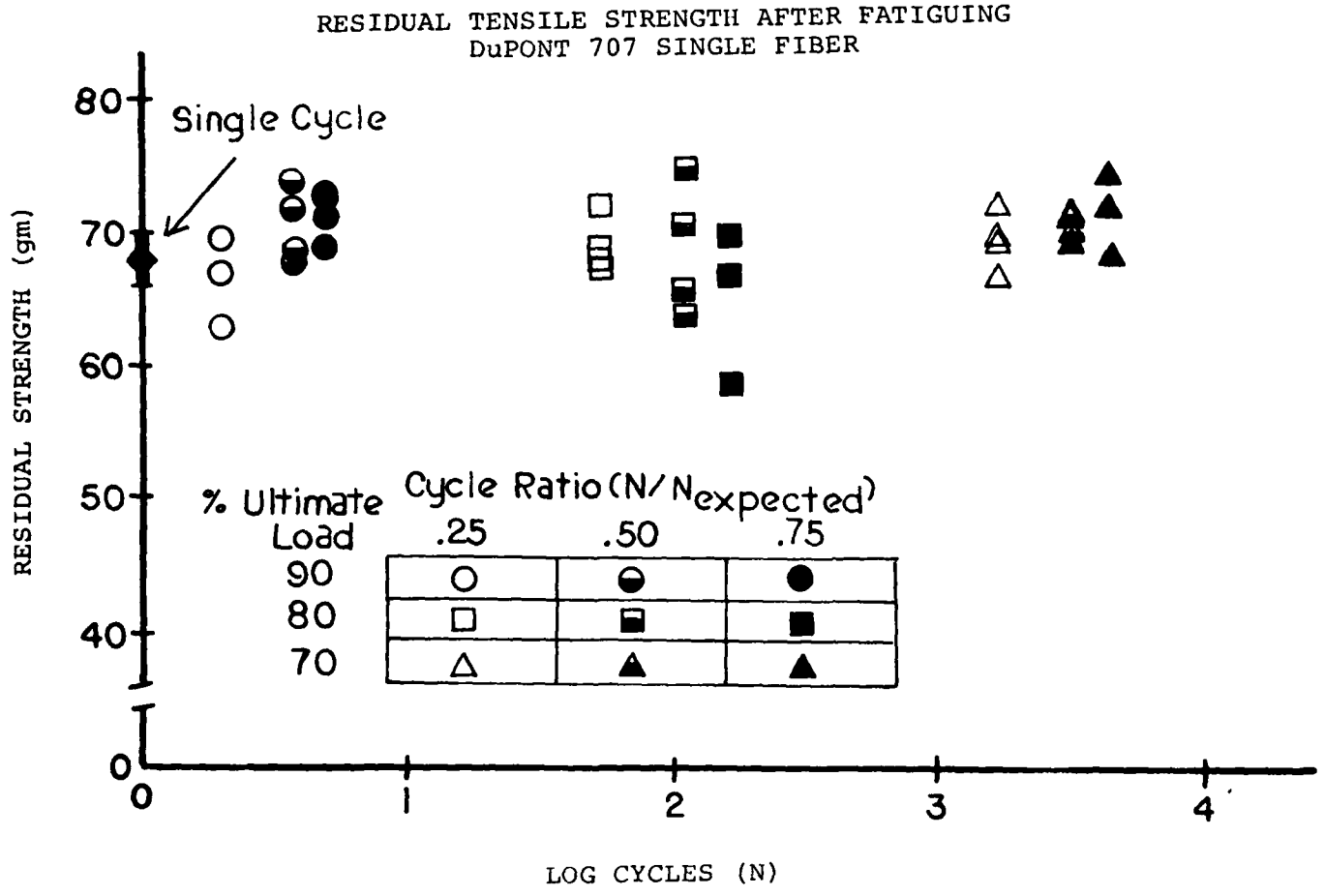
RESIDUAL TENSILE STRENGTH AFTER FATIGUING
DuPONT 707 SINGLE FIBER
RESIDUAL STRENGTH (gm)
80
70
60
50
40
0
Single Cycle
% Ultimate Load
Cycle Ratio (N/Nexpected)
.25
.50
.75
90
80
70
0
1
2
3
4
LOG CYCLES (N)

Figure 12

DuPONT 707 NYLON SINGLE FIBER
EXPERIMENTAL FATIGUE DATA COMPARED TO
PREDICTION FROM CREEP RUPTURE

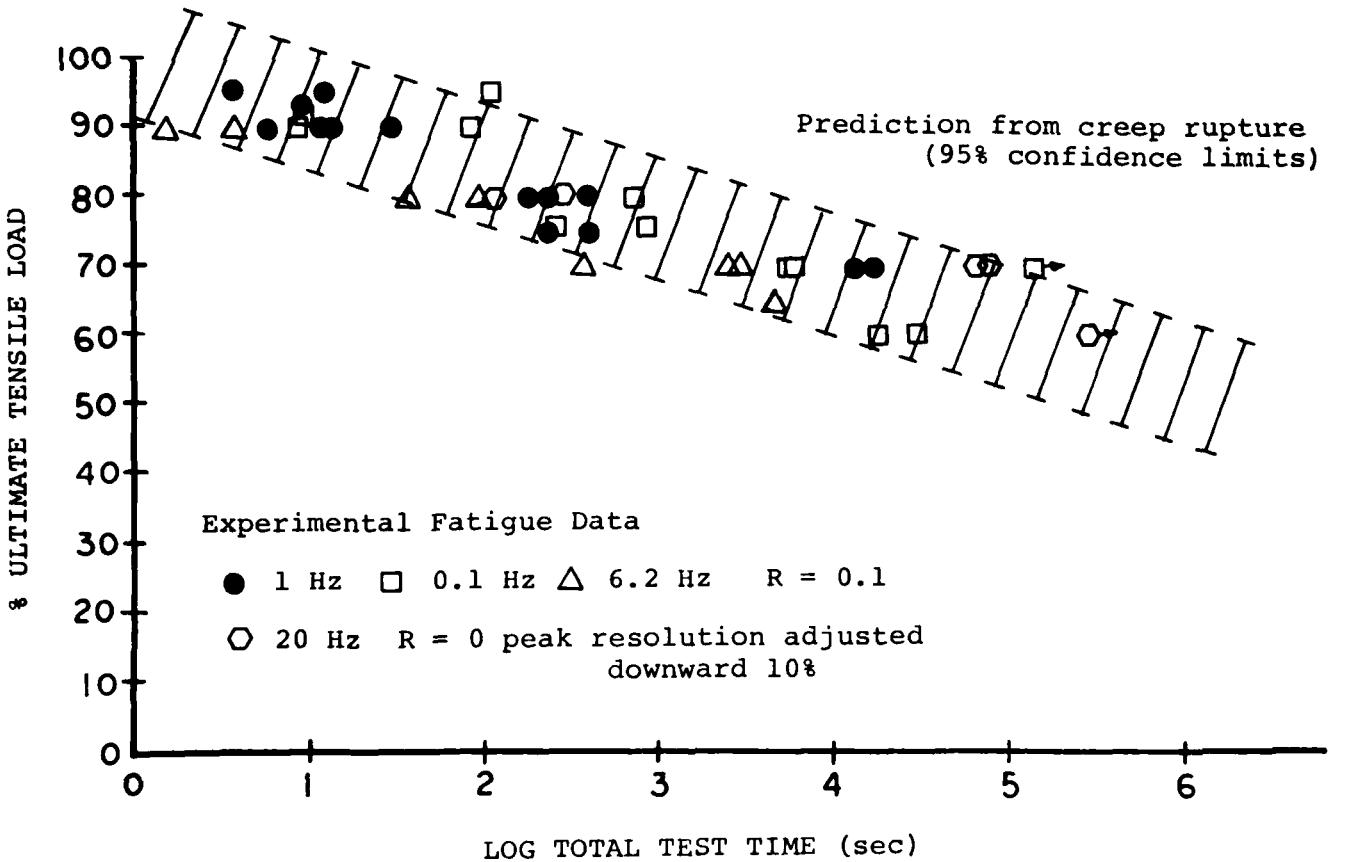

Figure 13

DuPONT 707 NYLON YARN
EXPERIMENTAL FATIGUE DATA COMPARED TO
PREDICTION FROM CREEP RUPTURE

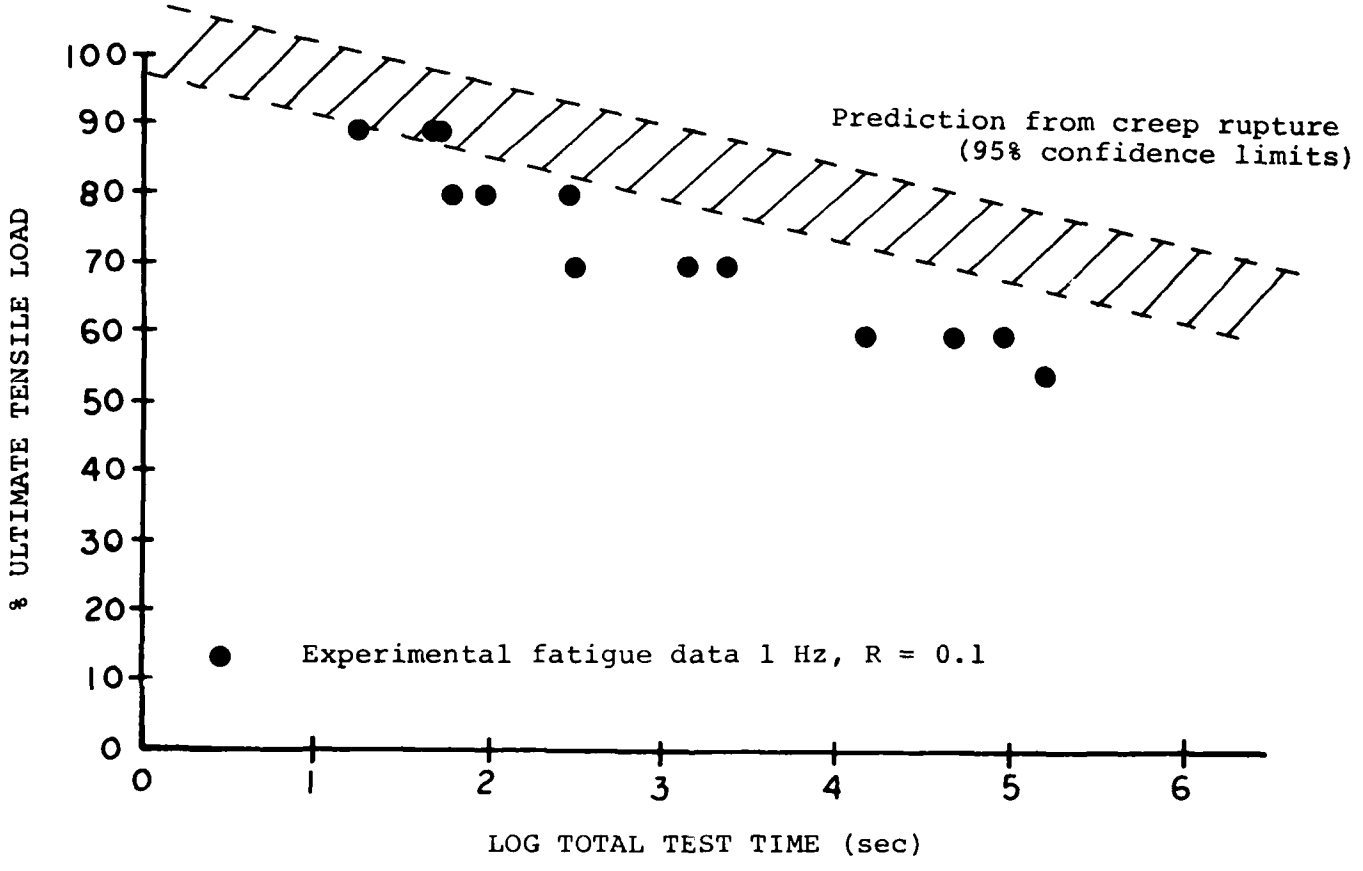

Figure 14

KEVLAR 49 SINGLE FIBER
EXPERIMENTAL FATIGUE DATA COMPARED TO
PREDICTION FROM CREEP RUPTURE

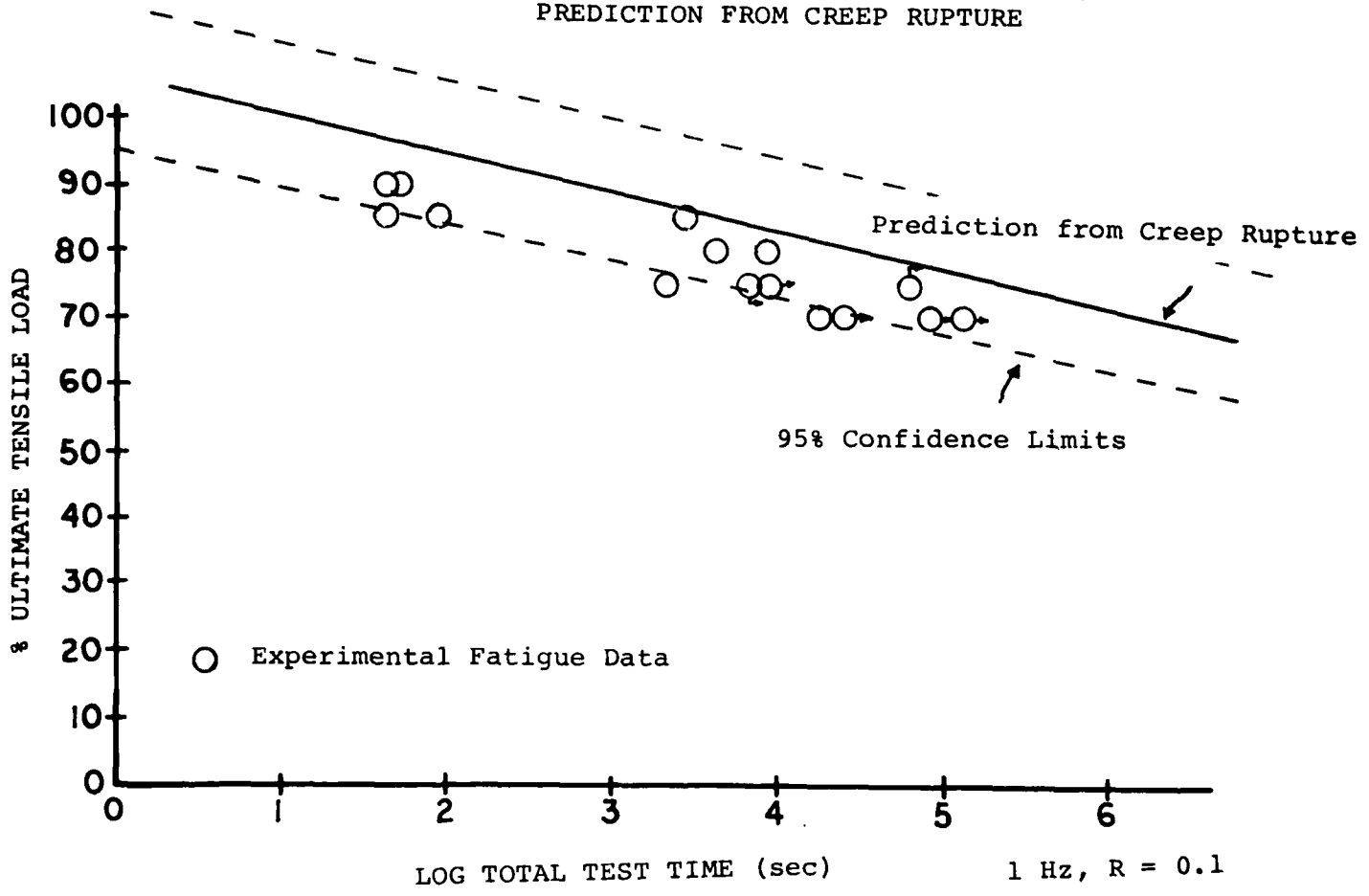

Figure 15

DuPONT POLYESTER SINGLE FIBER
EXPERIMENTAL FATIGUE DATA COMPARED TO
PREDICTION FROM CREEP RUPTURE

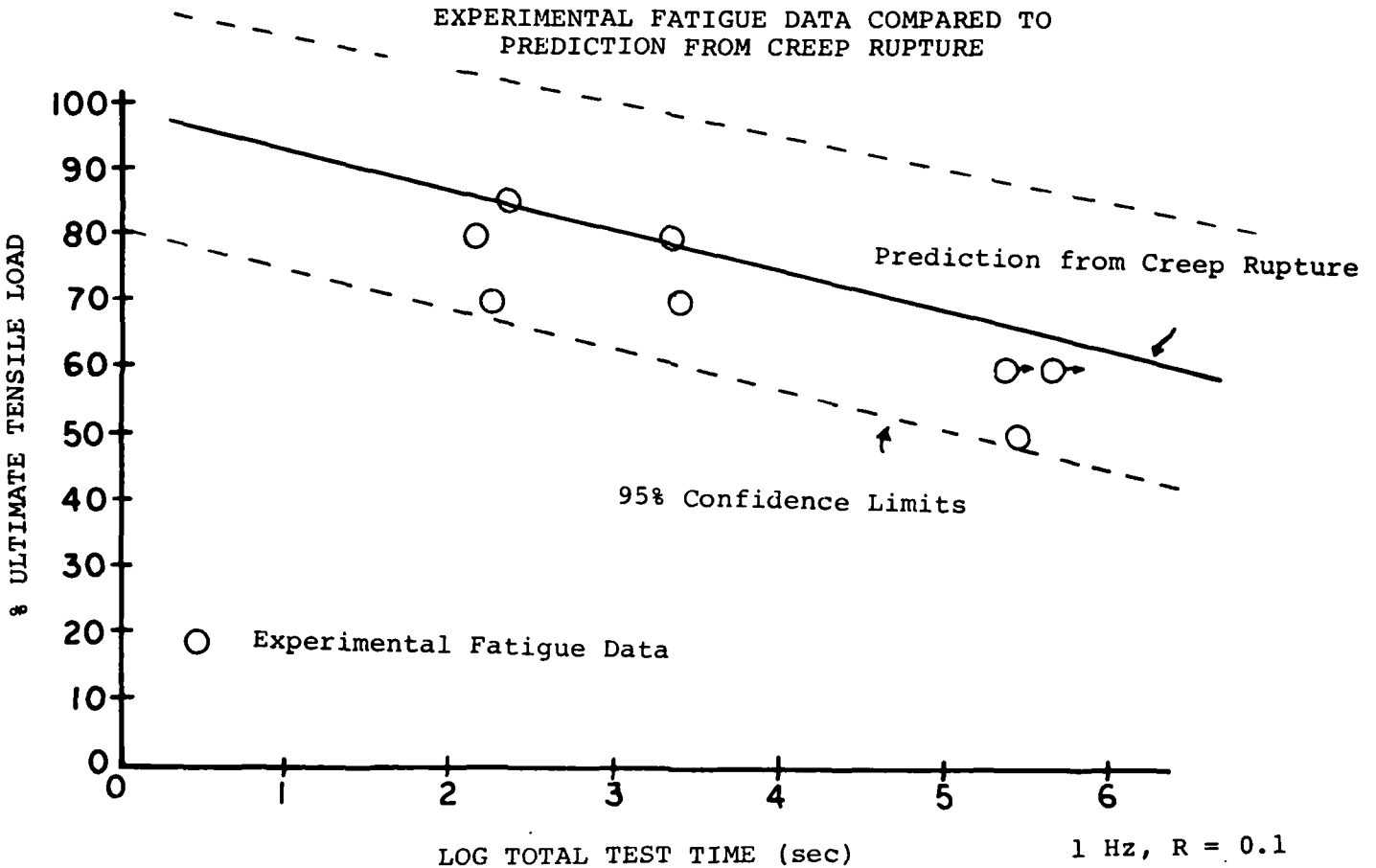

Figure 16

CREEP RUPTURE LIFETIMES
DuPONT 707 NYLON SINGLE FIBER, YARN, AND
3/16" DOUBLE BRAIDED ROPE

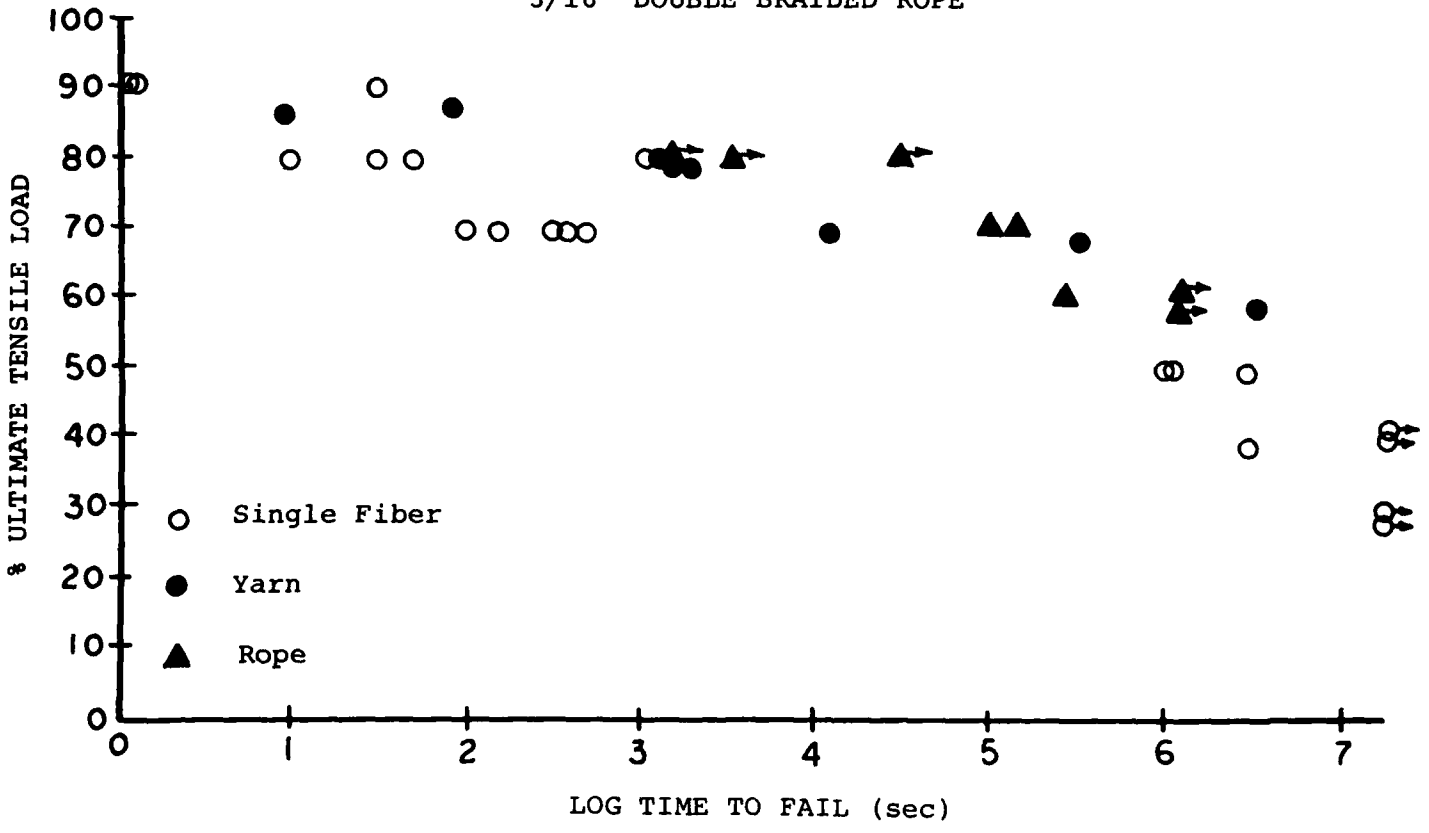

Figure 17

FATIGUE LIFETIMES
DuPONT 707 NYLON YARN AT VARIOUS R RATIOS

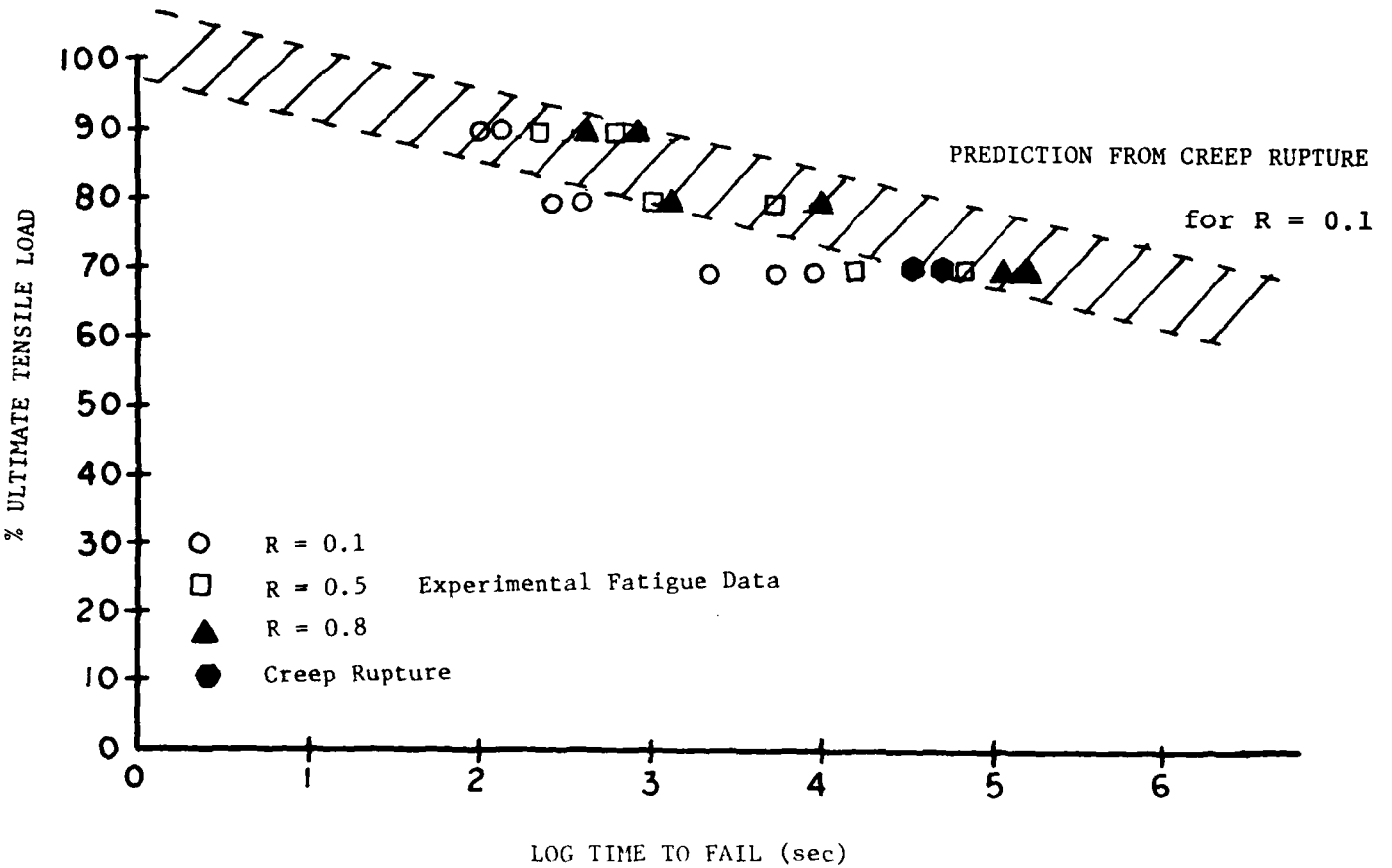

THE EFFECTS OF SEA WATER AND CONCENTRATED SALT SOLUTIONS ON THE FATIGUE OF NYLON 6,6 FIBERS

M.C. Kenney*, J.F. Mandell, F.J. McGarry

Department of Materials Science & Engineering
Massachusetts Institute of Technology
Cambridge, Ma. 02139 (USA)

SUMMARY

Cyclic fatigue and creep rupture tests have been run on high tenacity nylon 6,6 single fibers, yarns, and small ropes in air and sea water environments. Fatigue failure in each case is by a creep rupture mechanism; yarns and small ropes show the same fatigue sensitivity as do single fibers. Sea water reduces the strength by approximately 10% under most conditions. Concentrated metallic salt solutions which cause environmental stress cracking in bulk nylon do not degrade the fibers beyond the effect of plain water. Tests on oriented nylon specimens show that environmental stress crack sensitivity is greatly reduced by orientation.

Submitted to Fibre Science and Technology

*present address: Albany International Research Co., Dedham, MA 02026

INTRODUCTION

Many applications of nylon fibers include a complex history of environmental exposure and mechanical loading [1]. This work is concerned with nylon fibers used in marine rope, and with determining the mechanisms by which salt water environments combined with fatigue loading might cause weakening and failure. While literature on this subject is limited to a few studies of rope performance [2,3,4], there has been considerable interest in the areas of environmental stress cracking and moisture effects on the fatigue behavior of bulk nylon specimens.

Environmental stress cracking in polymers refers to crack-induced failure under tensile loads in the presence of an environmental agent which causes failure at stresses well below those that would otherwise be required [5]. The problem is generally associated with the interaction of the environmental agent with crazes in bulk polymers; specific chemical agents cause problems with specific polymers. Stress cracking of bulk nylon by salt solutions has been reported by several workers [6-9], but, thus far, no studies on nylon fibers have been reported. The proposed mechanisms of attack in bulk nylon involve weakening of the nylon structure by disrupting hydrogen bonding either by local plasticization and swelling (Type I salts), or dissolution of the nylon (Type II salts). Disruption of hydrogen bonds may also be caused by plain water.

Plasticization increases segmental mobility and reduces Young's modulus. Ultimate elongation generally increases in bulk specimens [10,11], but in more highly oriented film and

fiber specimens the increase may be quite small, only about 5%. The ultimate tensile strength of nylon fibers is reported to decrease about 15% in water [12]. The creep rate of bulk nylon increases with moisture, which can cause shorter failure times [10].

Few studies have combined environmental exposure and fatigue loading. One such study on bulk nylon showed a minimum fatigue crack growth rate at around 2% moisture, apparently due to embrittlement below this value and excessive softening above [13]. A study on fibers in tap water showed that strength and fatigue lifetime were both reduced by immersion; testing in this case involved biaxial rotation over a pin, which may be subject to additional complications [14].

Several studies on the behavior of nylon ropes in sea water have been reported. In one [4], strength decreased by 50% and strain to failure increased by 50%. Wet ropes were also reported in Ref. [2] to show greater elongation under equivalent loads, and immersion appeared to reduce heat buildup during cycling. However, no specific data were given.

In the present study, well characterized ambient fatigue data were first established, and then used as baselines for comparisons with subsequent environmental effects. Detailed data for fatigue effects in air have been presented in an associated paper, Ref. [15]. Emphasis in this study is on properties at the single fiber and yarn levels under creep and fatigue loading in salt solutions. Some results on small ropes and bulk materials are also reported.

EXPERIMENTAL PROCEDURES

Fatigue testing was conducted using closed loop servohydraulic machines. Most tests were run in the load control mode, using a sine wave function. Ultimate tensile load was evaluated using a ramp test to failure at a rate equivalent to the loading portion of the fatigue cycle. Fatigue testing was conducted to various percentages of this ultimate tensile load. The specimens were cycled between the maximum tensile load and one-tenth of this value, giving a stress ratio, R, of 0.1. Other details of the test procedure can be found in Ref. [15].

A master frequency of 1 Hz was used for most testing, master frequency referring to the frequency corresponding to cycling at 100% of ultimate tensile load. The actual test frequency at each percentage of ultimate tensile load was then adjusted upward to maintain a constant loading rate. Thus, the frequency was increased as the maximum load was decreased. Test frequency was kept as close as possible to this level, except where machine resonances required slightly lower values. The master frequency is given on each figure.

A cardboard tabbing system was used for testing of dry yarns and single fibers. A flexible silicone sealant was used at the tab end to improve stress transfer and protect the specimen from abrasion. Further into the tab a rigid adhesive (Eastman 910) was used. For sea water testing, a modified system was constructed of PVC tabs, sanded, thinned at the tip, and acetone cleaned prior to fiber bonding with Epon 828/TETA epoxy adhesive. Using this tabbing method, the majority of fiber breaks occurred in the gage section, away from the grips, considered

valid test results. For rope gripping, silicone and polyester adhesives were used to encapsulate rope ends into tapered metal fittings. The gage length between adhesive points for single fibers and yarns was five inches (127 mm); the gage length between fittings for small ropes was four inches (102 mm).

Control tests for comparison with various environments were run dry, in laboratory air. The ambient conditions were air conditioned without humidity control for all tests with the exception of single fiber creep rupture tests which were run at 65% RH in a chamber. Possible effects of varying ambient humidity were investigated by conducting a series of yarn creep rupture tests at 65% RH and in ambient air, the latter tests covering both summer and winter conditions. Creep rupture lifetimes were virtually identical for the two test series over the complete load range of interest, giving lifetimes from 10 to 10^7 seconds. Thus, ambient air tests give results representative of a constant 65% RH over the lifetime range discussed in this paper.

ASTM standard formulation D1141 was used for sea water composition [16]. A specially designed plastic chamber and grips were used for sea water fatigue of single fibers and yarns. During cycling the chamber is mounted on the testing machine piston and moves up and down around a freely traveling rod attached to the load cell. This configuration is necessary when using sensitive load cells which cannot support the weight of the chamber. Careful adjustment of the electronic gain is required for smooth operation, and the upper grip must remain above water to avoid control problems from hydrodynamic effects. For small rope testing, a large plastic tube system was used with tap

water flowing through the apparatus constantly.

Creep rupture lifetimes for fibers and yarns were measured using a dead load arrangement. Environmental exposure during creep rupture was accomplished by enclosure in small heat-sealed plastic bags left open at the top for access.

In environmental tests on bulk nylon tensile bars, a small cup was formed on the (vertical) specimen surface using a bead of RTV silicone, and several drops of the environmental agent were applied. Several such cups could be formed on each specimen. Except for very short lifetime tests, the specimen was loaded for approximately 30 seconds prior to application of the agent, as is commonly done [7,8]. The control condition used plain water in one of the cups on the specimen. In all cases where failure was observed, the section containing the environmental agent was the source of the failure.

The primary material was DuPont 707 nylon 6,6 yarn, a standard rope yarn used commercially. The yarn consists of 210 lightly interlaced fibers producing a total of 1260 denier taken from a single lot and merge. Single 30μm fibers for testing were carefully extracted from sections of this yarn. The small rope used was 3/16 inch diameter double braided, based on DuPont 707 nylon yarn, purchased from Sampson Ocean Systems.

Three types of bulk specimens were used to study the effect of increasing degrees of orientation. These were, in order of increasing orientation, specimens machined from large center-gated injection molded plaques (surfaces removed), end-gated injection molded tensile bars, and specimens cold drawn from

molded tensile bars. Drawing was conducted at a slow rate (2 mm/min) on a universal testing machine at room temperature. The draw ratio was determined by the change in cross-sectional area, ranging from 2.59 to 2.83. Moisture content prior to testing was 1.4% for the machined plaques and 2.0% for the tensile bars.

RESULTS AND DISCUSSION

Fatigue in Sea Water

S-N data for short term sea water exposure of single fibers and yarns are shown in Figures 1 and 2. These tests were conducted on specimens immersed in sea water for five minutes before testing. (Longer exposure times will be discussed later.) The load coordinate on each plot is normalized by the single cycle ultimate tensile load at the conditions of that particular data set. Values of ultimate tensile load are given in Table 1 and can be used to determine absolute load values for the S-N data. Because of machine resonances with the sea water chamber, single fiber data were run in the range of 0.6 to 1.0 Hz and yarn data in the range of 1.1 to 1.2 Hz.

The effects of sea water immersion during fatigue are relatively mild. Lifetimes at the lower stress levels in sea water are displaced from those in air by less than one decade shorter lifetime or 10% lower (normalized) load. Although a ten-fold decrease in lifetime is significant, it represents only a small shift in the failure load. This does not appear sufficient to be a dominant factor in those service failures which occur at relatively low loads. The initial ultimate tensile load for the fibers, as given in Table 1, also drops by about 10%, as has

been observed in the literature [12]. Initial ultimate tensile load for the yarn increases very slightly on short term sea water exposure. This may be explained by a lubricating effect of the water, which allows fibers within the yarn to align in a more nearly parallel, more efficient, structure.

S-N data for short term tap water exposure of a limited number of specimens of small rope are shown in Figure 3. The wet and dry rope data are similar to those of the other structures; the S-N data in sea water are reduced to about 10% lower load or one decade shorter lifetime. In this case, however, both the wet and dry rope data are normalized to the initial strength of the dry rope, and run at 0.5 Hz. Grip failures became a problem at lower loads, and are shown in Figure 3 by points with arrows, representing the lowest possible lifetime for gage section failure.

Sea water results for single fibers, yarns, and small ropes are compared in Figure 4. The results are plotted as a function of log time rather than cycles to account for differences in the frequencies used. Single fiber and yarn data are approximately linear, with similar slopes, and nearly superimpose on a normalized scale. This can also be seen from comparison of the regression equations, where 95% confidence limits are given in parentheses:

$$\text{single fiber: } P/P_{ult} = 1.03\ (\pm.044) - .103(\pm.003)\log N$$

$$\text{yarn: } P/P_{ult} = .972\ (\pm.03) - .111(\pm.002)\log N$$

where P is the load and N is cycles to failure. Small rope data are generally similar to those of single fibers and yarns, but the occurrence of many grip failures limits the significance of

comparisons. The similarity of normalized data among the various structures indicates a common factor in their fatigue degradation, as has also been shown in Ref. [15] for dry structures.

The associated paper [15] on fatigue in air is considered the origin of the cyclic fatigue behavior. It was shown that a creep rupture based model could accurately predict the cyclic fatigue lifetime over a range of conditions. Compared with a constant maximum load in a creep test, cycling to lower loads while maintaining the same maximum load simply extends the total time to failure by reducing the time at high loads. Failure was shown to occur at a particular cumulative strain for each level of structure regardless of the type of loading. Over a broad range of frequency, failure occurred at a particular total test time, independent of the number of cycles.

Figures 5 and 6 give creep rupture data for single fibers and yarns in sea water and air, and in other environments which will be discussed later. The load data in Figure 6 are normalized by the UTS in that environment from a ramp test having a failure time of approximately 0.5 seconds (Table 1), while the data in Figure 5 are not normalized (the ramp values are indicated on the load coordinate). Creep rupture lifetimes for the single fibers are generally similar in air and sea water, at the same load. For yarns, the creep rupture curve in sea water falls at 10-15% lower load than that in air, but has a similar trend. The yarns have about the same strength in sea water and air (Table 1) despite the lower individual fiber strength in sea water; this is apparently the result of a greater bundle efficiency in water,

possibly due to a lubricating effect. Thus, the effect of sea water on the yarn creep rupture curve may not be due to a different response to creep, but only to the initial ramp strength used to normalize the data; the dry strength (and creep rupture) are complicated by broken fibers which only partially unload [15].

The creep rupture data in Figures 5 and 6 have been used to predict the cyclic fatigue response through the model described in Ref. [15]. Figures 7 and 8 show that the cyclic data are in general agreement with the lifetime ranges predicted from creep rupture. In fact, the wet yarn data are in better agreement than those tested under dry conditions [15]. The water environment apparently lubricates the yarn and precludes commplications from broken fiber reloading observed in the creep rupture behavior of dry yarns. Figures 7 and 8 clearly demonstrate that the cyclic fatigue of nylon 6,6 single fibers and yarns in sea water as in air is due to a creep rupture mechanism. Table 2 shows that the cumulative strain to failure is the same whether the tests are creep rupture, cyclic fatigue, or simple ramp tension, also consistent with the creep rupture model.

Effects of Preconditioning Under Load

The fatigue data in Figures 1-3 are for tests with only a 5-minute preconditioning time in sea water. Selected tests have also been run with longer preconditioning while under a dead load. For yarn specimens immersed in sea water for one month at dead loads of 14% and 3% of the wet yarn strength, and for control specimens immersed unloaded, a very slight decrease in

ramp tensile strength with increasing applied load during conditioning was observed. The strength decreased from 11.99 kg in the unloaded case to 11.47 kg for the 14% loading (Table 3). However, the overall effect is minimal, and traditional environmental stress cracking does not appear to occur on this time scale. Specimens loaded at 3% in air for one month showed a slight increase in tensile strength. This effect is attributed to an initial structural alignment in the yarn, as similar increases are observed in specimens loaded for only five minute periods. Several specimens were also soaked in sea water and allowed to dry; this was repeated three times in succession with no adverse effects on dry strength.

Fatigue data obtained after the four types of one month conditioning are plotted in Figure 9. All sea water behavior, including the original five minute immersion data, fall on approximately the same line. Clearly, there is no significant effect of this conditioning on fatigue or strength. Data from specimens which were preloaded and tested dry also follow the original dry S-N curve.

In view of the minimal effects observed after one month of sea water conditioning, a considerably longer period of immersion under load was studied. After immersion for ten months under 19% of ultimate load, failure at or quite near the grips during subsequent testing was a problem; however, even these tests gave an average strength of 80% of the initial strength.

Effects of More Severe Stress Cracking Agents

The standard sea water solution is very dilute and the components relatively inactive when compared to the aqueous solutions of certain salts which have been reported to stress crack bulk nylon [7,8]. To further investigate environmental sensitivity, series of tests were conducted in more potent stress crack agents: solutions of LiBr (40% w/v) and LiCl (20% w/v). Saturated solutions of these salts have been reported to crack bulk nylon within several minutes to 48 hours [7,8]. In the current tests, specimens were immersed in the solutions at several load levels, and creep rupture lifetimes were recorded. Yarn results, plotted in Figure 6., show that LiCl, LiBr, and also plain deionized water have exactly the same effect as standard sea water, showing approximately 10% lower loads or about one or two decades shorter lifetimes compared with dry specimens. The common behavior observed in all aqueous solutions clearly shows that the dominant factor is the aqueous environment, with no measurable effect of the other constituents. It appears that the process is controlled by simple plasticization, as has been observed for nylon in an aqueous environment [10]. Tests on single fibers (Figure 7) gave similar results.

Effects of Moisture on Stress-Strain Behavior

The effects of water on nylon under the conditions of this study appear to be a simple plasticizing action. Figure 10 gives simple constant displacement rate stress-strain curves of yarns in ambient air and in sea water after a five minute

conditioning period (the rate is equivalent to a 1 Hz test). The effect shown is completely reversible: if the yarn is immersed and then redried, the original dry stress-strain curve is again obtained. The initial modulus of the yarn in water is only 38% of the value in ambient air, while the remainder of the stress-strain curve and the failure conditions are much less affected. Tests on single fibers and yarns after as much as four months immersion in sea water show no further reduction in modulus beyond the effect at five minutes.

Effects of Orientation on Environmental Stress Crack Resistance

Textile fibers appear to be less susceptible to stress cracking agents than are bulk nylon specimens. The effect of orientation was studied directly using bulk nylon 6,6 specimens containing varying amounts of orientation produced by methods described earlier. Wide angle X-ray diffraction patterns of the three bulk specimen types are shown in Figure 11. The two molded, undrawn specimens show little orientation; they differ primarily in surface orientation, which is not distinguishable in diffraction patterns averaged through the thickness. Cold drawn tensile bars show a notably increased orientation, indicated qualitatively by the bright diffraction spots as compared with uniform rings for the unoriented materials. Test results for bulk specimens are summarized in Figure 12. Ultimate tensile strengths were determined for each specimen type, and stress cracking tests were conducted at various percentages of the ultimate. Ultimate tensile strength, based on the initial cross-sectional area after drawing, ranged from 10,900 to 29,000 psi (75.1 to 205 MPa) for the three increasing levels of orientation. For the machined plaques, failures with the cracking agent present were brittle at all load levels, apparently from

crazing induced by the LiBr solution. All failure times are actually quite long (greater than 2500 seconds), showing that even in this aggressive environment the bulk specimens do not degrade rapidly. The failure times were longer than in reported studies [7], possibly the result of differences in specimen type and test conditions.

The injection molded bars show consistently longer failure times than do the machined plaques, except at high stresses where ductile failure becomes the dominant mode. For the drawn specimens, failure times are still longer, both at the same absolute stress level and at an equivalent percentage of ultimate tensile strength. Drawn specimens crazed or cracked extensively, but did not separate.

It is apparent that increasing amounts of orientation are effective in suppressing environmental stress cracking. Therefore, high tenacity fibers of even greater orientation and ultimate tensile strength would be expected to show still less sensitivity to stress cracking agents. Long term tests on fibers, still in progress, show no evidence of environmental stress cracking after two years at 40% of ultimate load.

The suppression of environmental stress cracking can be understood in terms of the fiber structure and mechanism of cracking. Conventionally, environmental stress cracking occurs by formation of a craze perpendicular to the stress direction, which allows subsequent penetration of the environment by capillary action [17, 18, 19]. Orientation of polymer chains parallel to the fiber axis, and thus the stress direction, makes formation of perpendicular crazes increasingly difficult. Crazes, if formed at all, must occur parallel to the stress

direction in a much more difficult process. Some examples of crazes of this type have been observed in the literature [20]. In the tests on fibers reported here, only one case of crazing has been found; this apparent craze runs parallel to the fiber axis, as shown in Figure 13. The suppression of crazing has also been reported to decrease susceptibility to stress cracking in other bulk polymers [21].

CONCLUSIONS

Immersion in sea water during fatigue or creep loading reduces the strength of nylon 6,6 single fibers, yarns, and small ropes by approximately 10% in most cases, as compared with an ambient air environment. Failure under cyclic loading correlates with lifetime predictions from a creep rupture based model. Concentrated solutions of LiCl and LiBr, which cause environmental stress cracking in bulk nylon, have no effect on fibers beyond the effects of pure water. The increased resistance of fibers results from orientation introduced during drawing from bulk to fiber form.

ACKNOWLEDGEMENT

This research is part of a broad study of the deterioration of synthetic marine rope supported by the Naval Sea Systems Command through the MIT Sea Grant Program. Mr. George Prentice is the Navy's technical liaison person on the project.

REFERENCES

1. N. Starsmore, M.G. Halliday, W.A. Ewere, "Proc. Int. Symp. Ocean Engr.-Ship Handling," Gothenberg, Sweden (1980) paper 13.

2. W. Paul, USCG Academy, New London CT, Govt. Report ADA 084 622 (1970) 2.1.

3. J.F. Flory, F.A. Denham, J.T. Marcello, P.F. Poranski, S.P. Woehleke, USCG Report CG-D49-77 (ADA 050 1829), (1977) 5.1.

4. K.R. Bitting, USCG Report CG-D-39-80 (ADA 087 106), 1980.

5. E.J. Kramer, "Developments in Polymer Fracture," E.H. Andrews, ed., Applied Sci. Publishers Ltd., London (1979).

6. R.P. Burford, D.R.G. Williams, J. Mat. Sci. 14 (1979) 2872.

7. P. Dunn, G.F. Sansom, J. App. Poly. Sci. 13 (1969) 1641.

8. P. Dunn, G.F. Sansom, J. App. Poly. Sci. 13 (1969) 1657.

9. A.C. Reimschuessel, Y.J. Kim, J. Mat. Sci. 13 (1978) 243.

10. M.I. Kohan, ed., "Nylon Plastics," Wiley, New York (1973).

11. H.W. Starkweather, "Water in Polymers," S.P. Rowland, ed., ACS Symp. Ser. No. 127 (1980) 433.

12. W.E. Morton, J.W.S. Hearle, "Physical Properties of Textile Fibers," John Wiley and Sons, New York, 1975.

13. P.E. Bretz, R.W. Hertzberg, J.A. Manson, J. Mat. Sci. 14 (1979) 2482.

14. J.W.S. Hearle, B.S. Wong, J. Tex. Inst. 68 (1977) 127.

15. M.C. Kenney, J.F. Mandell, F.J. McGarry, "Fatigue Behavior of Synthetic Fibers, Yarns, and Ropes," submitted to Fibre Science and Tech (1984).

16. Standard Specification for Substitute Ocean Water D1141-75, 1979 Annual Book of ASTM Standards, Part 31, Water, American Society for Testing and Materials, Philadelphia, PA, 949.

17. R.P. Kambour, "Mechanisms of Environment Sensitive Cracking of Materials," P.R. Swann, F.P. Ford, A.R.C. Westwood, eds., The Metals Society (1977) 213.

18. R.A. Bubeck, Polymer 22 (1981) 682.

19. G.P. Marshall, L.E. Culver, J.G. Williams, Proc. R. Soc. Lond. A 319 (1970) 165.

20. A. Garton, D.J. Carlsson, R.F. Stepaniak, D.M. Wiles, Poly. Eng. Sci. 18 (1978) 923.

21. R.P. Kambour, J. Poly. Sci.: Macromolec. Reviews 7 (1973) 1.

Table 1

ULTIMATE LOAD AND ELONGATION IN

SINGLE CYCLE RAMP TESTS

		Ultimate* Load	Ultimate* Elongation (%)
FIBER	Air	68.1 gm (± 2.0)	15.0 (± .75)
	Sea Water	60.4 gm (± 3.2)	14.4 (± 1.2)
YARN	Air	11.61 kg (± .43)	17.0 (± 1.4)
	Sea Water	12.11 kg (± .26)	17.8 (± 1.4)
ROPE	Air	605 kg (± 21)	40.9 (± 2.0)

* approximate failure time = 0.5 sec.

Table 2

COMPARISON OF ELONGATION AT BREAK

FOR SINGLE CYCLE RAMP, FATIGUE, AND CREEP TESTS.

		Cumulative Strain to Failure (%)		
		Ramp	Fatigue*	Creep*
FIBER	Air	15.0 (± .75)	14.6	14.4
	Sea Water	14.4 (± 1.2)	14.5	14.9
YARN	Air	17.0 (± 1.4)	18.9	18.9
	Sea Water	17.8 (± 1.4)	17.6	----
ROPE	Air	40.9 (± 2.0)	41.9	41.4

* single specimen at 70% of ultimate load, typical data.

Table 3

RESIDUAL ULTIMATE STENGTH AND ELONGATION OF DuPONT 707 NYLON YARN AFTER ONE MONTH CONDITIONING

Conditioning Load, Environment	Ultimate Load (kg)	Elongation (%)
Unloaded, sea water	11.99 (± .20)	21.8 (± .5)
1.7 Kg, sea water	11.47 (± .29)	17.4 (± .4)
0.4 Kg, sea water	11.65 (± .28)	18.3 (± 1.0)
0.4 Kg, air	12.40 (± .49)	16.2 (± .9)

FIGURE CAPTIONS

Fig.	Caption
1	S-N Fatigue Data for Single Nylon Fibers in Air and Sea Water.
2.	S-N Fatigue Data for Nylon Yarns in Air and Sea Water.
3.	S-N Fatigue Data for 3/16 in. Nylon Double Braided Rope in Air and Tap Water (Normalized by Dry Ultimate Load).
4.	Comparison of Fatigue Data for Single Fibers, Yarns, and Ropes in water.
5.	Comparison of Creep Rupture Data for Single Fibers in Several Environments.
6.	Comparison of Creep Rupture Data for Yarns in Several Environments.
7.	Predicted vs. Experimental Fatigue Data For Single Fibers in Sea Water.
8.	Predicted vs. Experimental Fatigue Data for Yarns in Sea Water.
9.	Fatigue Data for Yarns After One Month Conditioning Under Several Loads and Environments.
10.	Typical Stress-Strain Curves For Yarns in Ambient Air and Sea Water After 5-minute Conditioning.
11.	Wide Angle X-Ray Diffraction Patterns of Bulk Nylon Tensile Bars at Three Levels of Orientation.
12.	Environmental Stress Cracking in LiBr Solution For Bulk Nylon at Three Levels of Orientation.
13.	Craze Structure Parallel to Axis of Fiber Exposed to LiCl Solution (20% w/v)

Figure 1

FATIGUE LIFETIMES
DuPONT 707 SINGLE FIBER IN SEA WATER AND AIR

1 Hz, R = 0.1

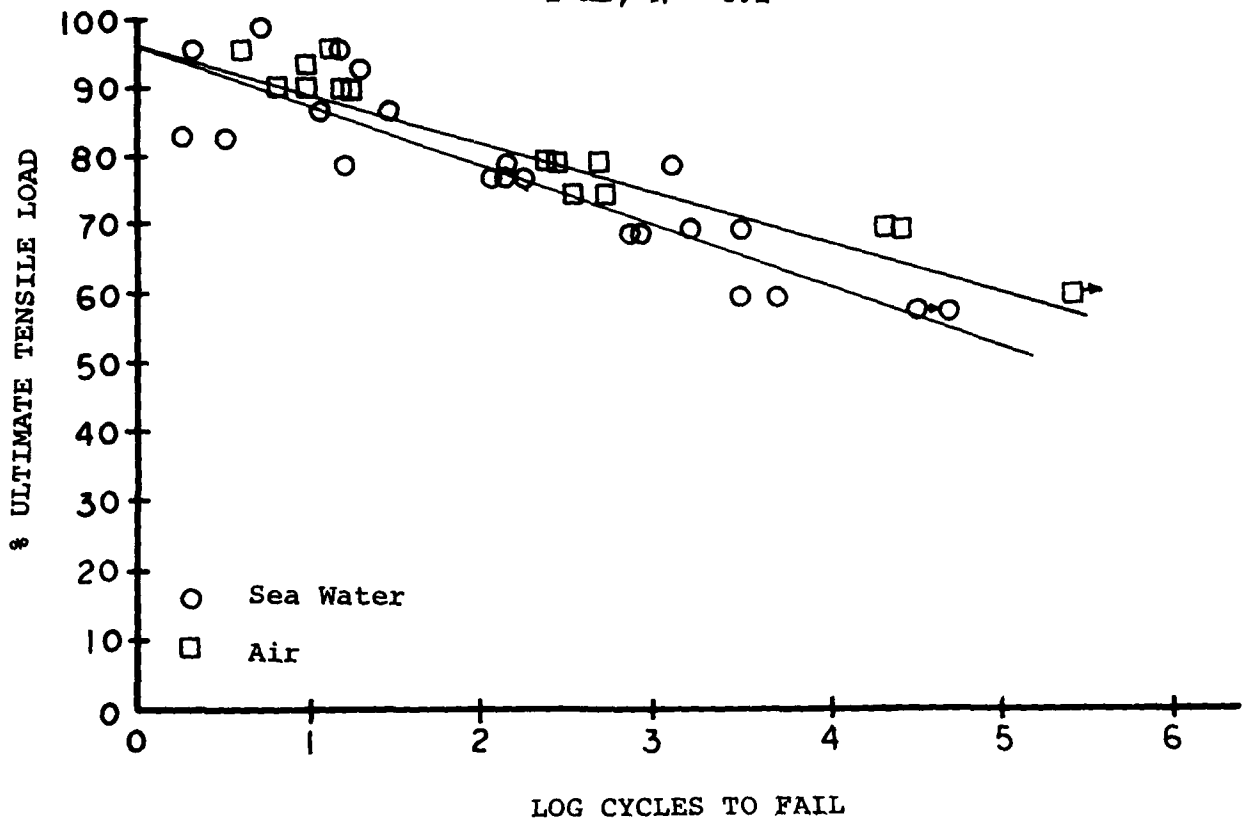

Figure 2

FATIGUE LIFETIMES
DuPONT 707 NYLON YARN IN SEA WATER AND AIR

1 Hz, R = 0.1

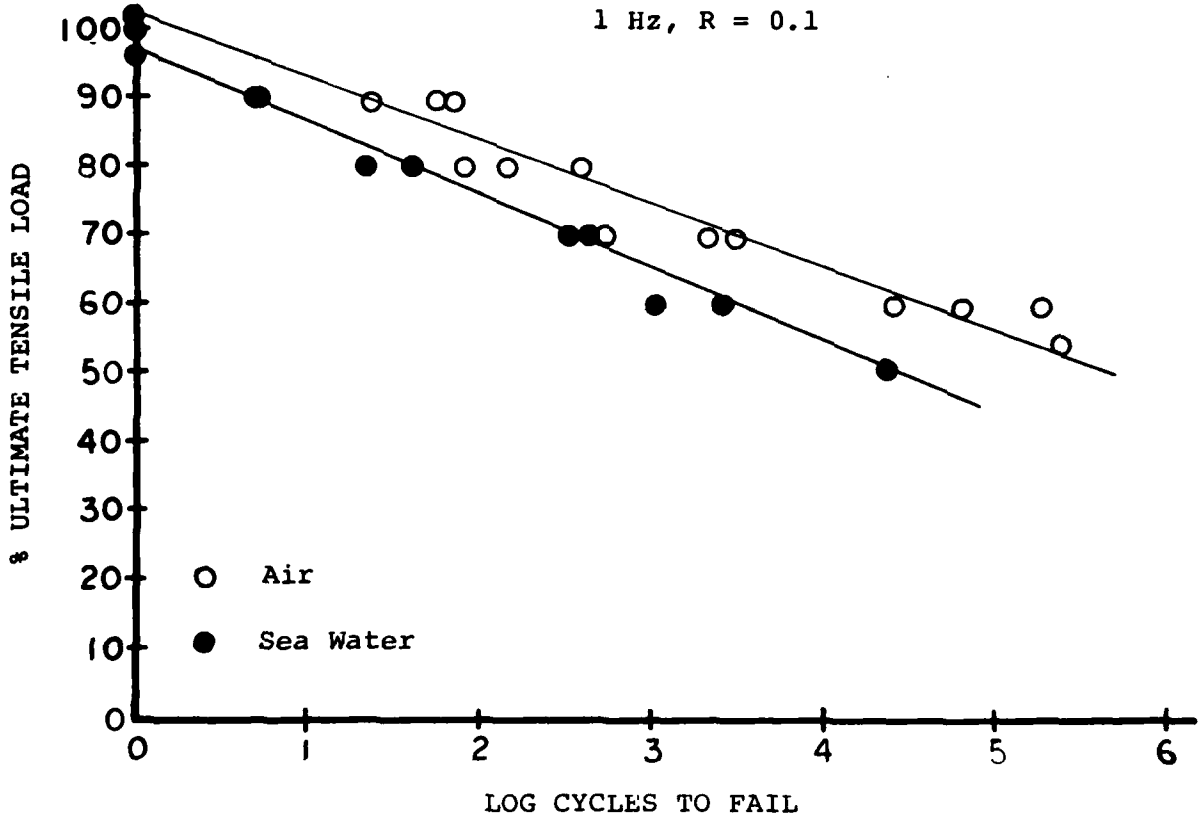

Figure 3

FATIGUE LIFETIMES 3/16" DOUBLE BRAIDED ROPE
IN AIR AND WATER

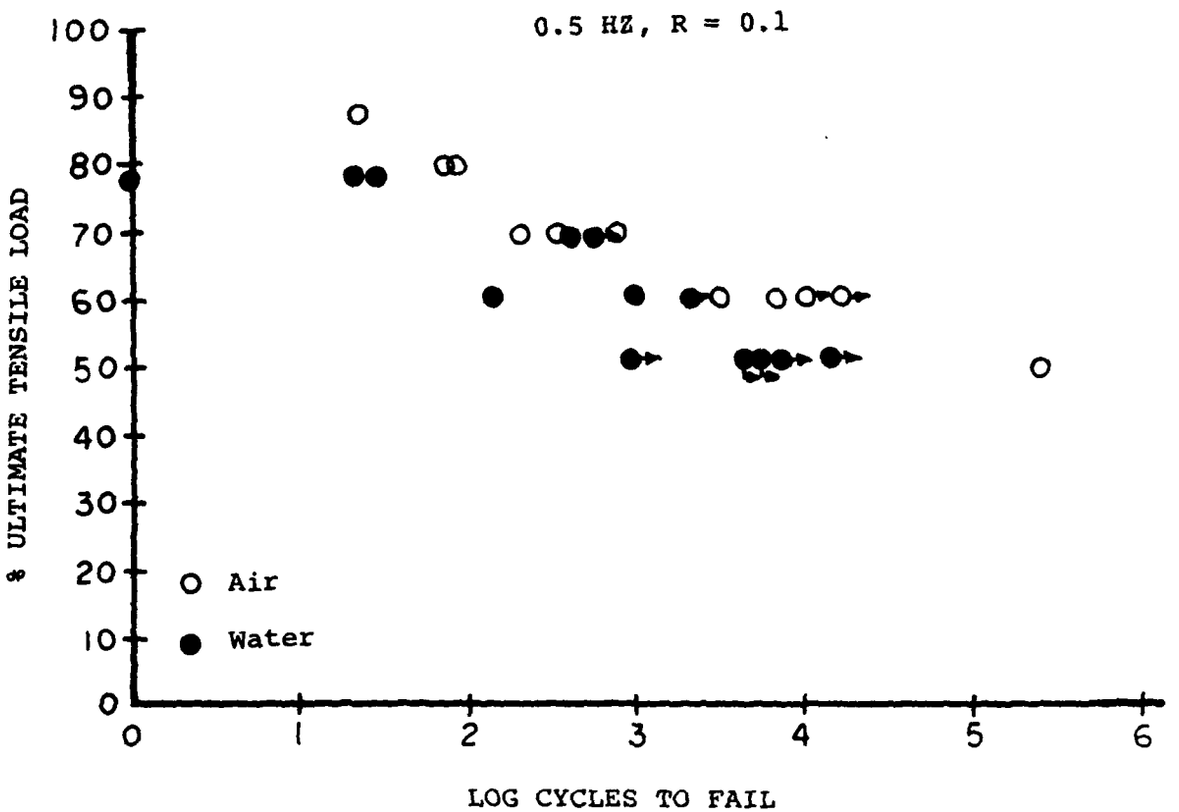

Figure 4

FATIGUE LIFETIMES DuPONT 707 NYLON SINGLE FIBER, YARN, AND 3/16" DOUBLE BRAIDED ROPE IN SEA WATER

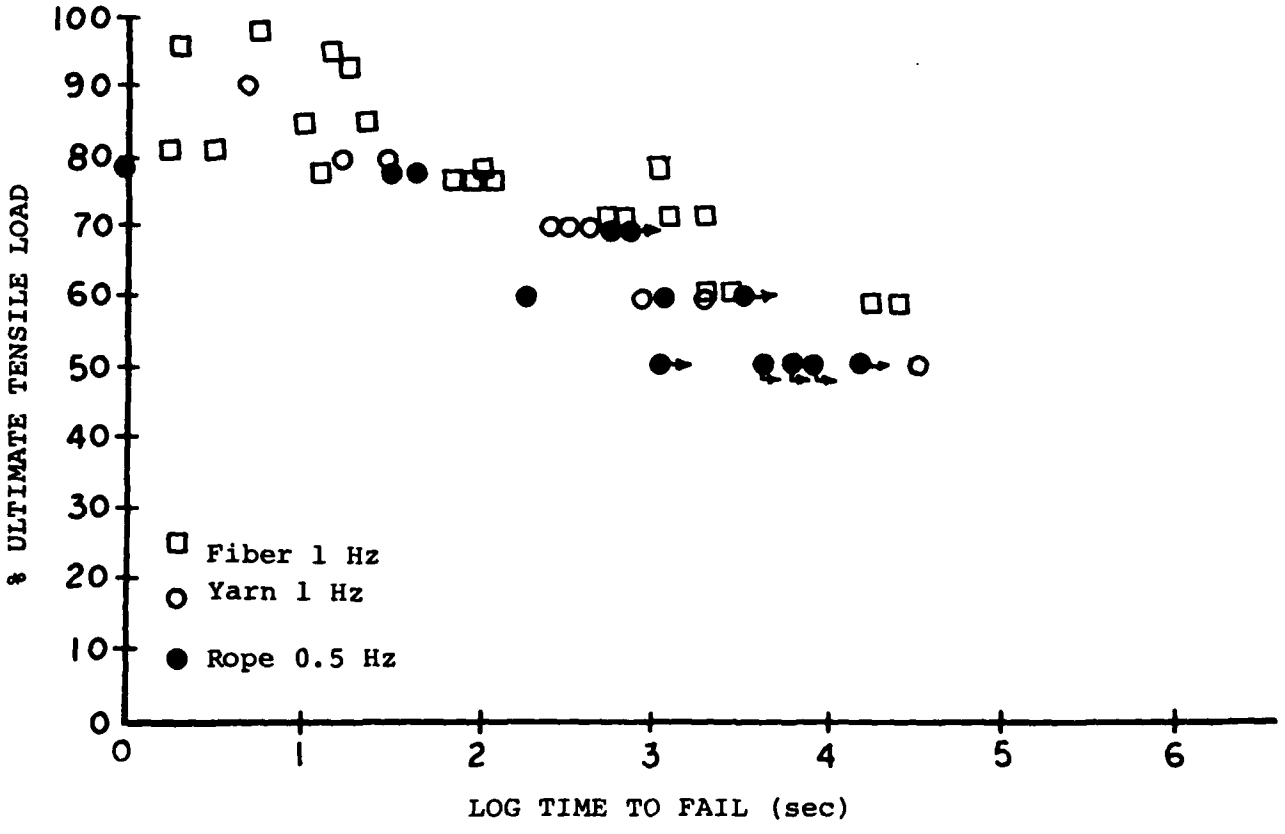

Figure 5

COMPARISON OF CREEP RUPTURE LIFETIMES
DuPONT 707 SINGLE FIBER IN SEVERAL ENVIRONMENTS

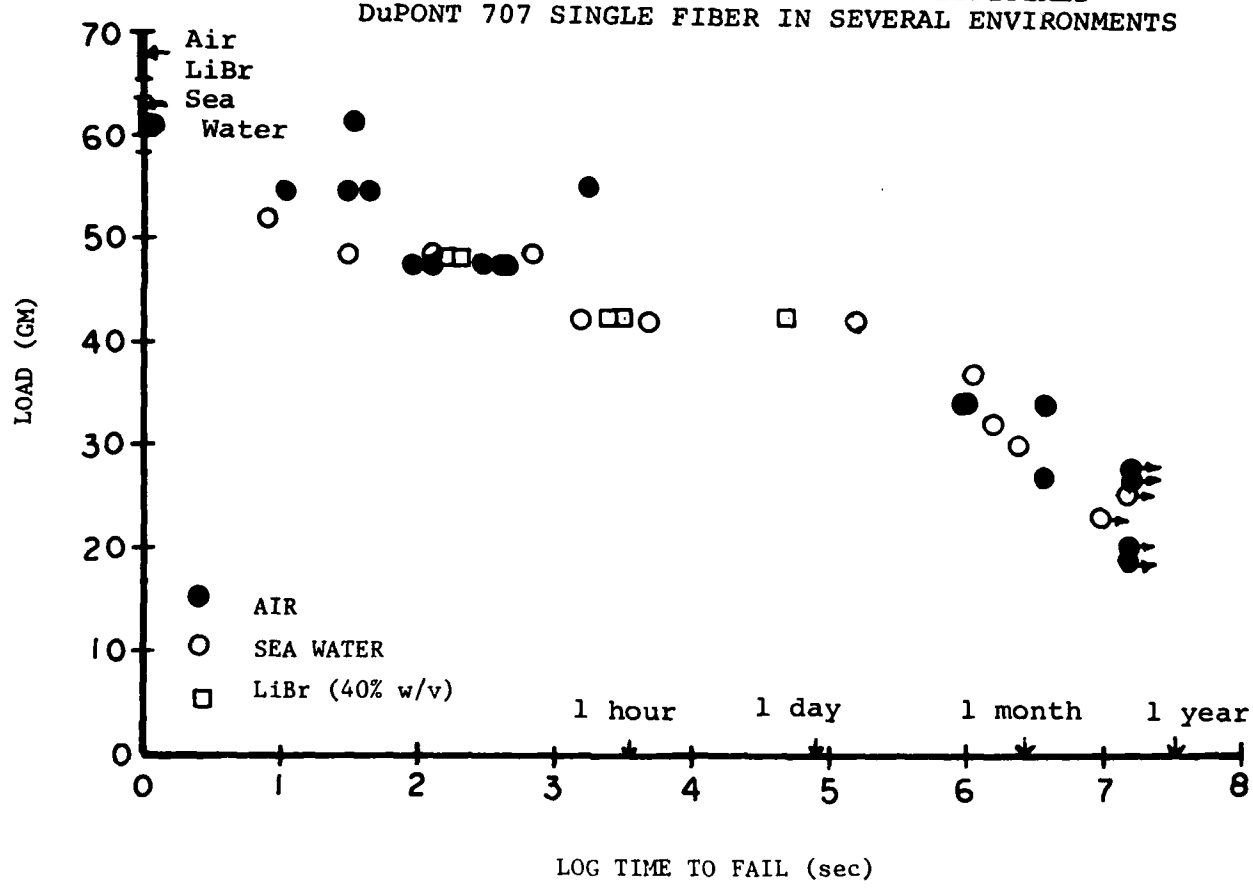

Figure 6

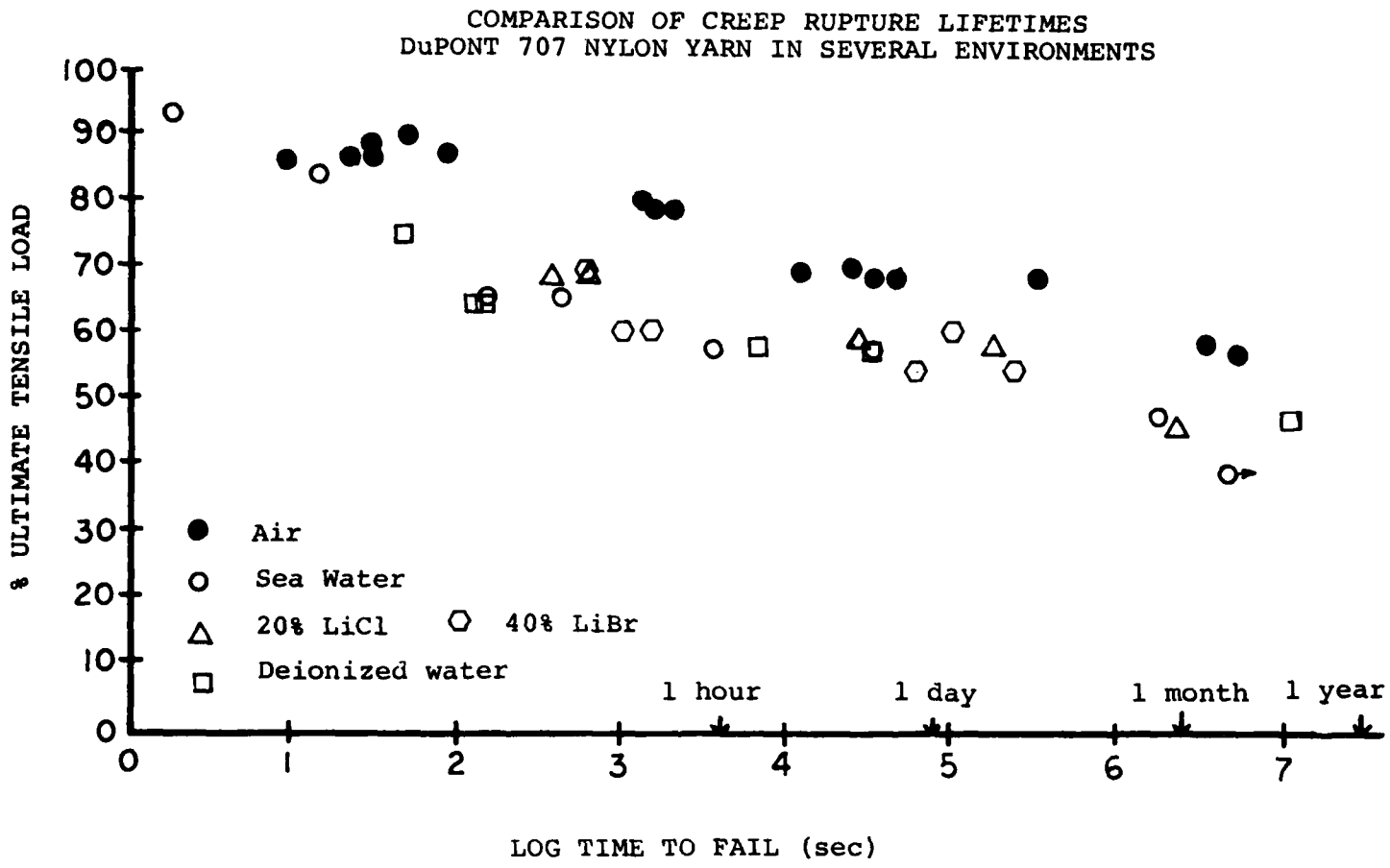
COMPARISON OF CREEP RUPTURE LIFETIMES
DuPONT 707 NYLON YARN IN SEVERAL ENVIRONMENTS
% ULTIMATE TENSILE LOAD
100
90
80
70
60
50
40
30
20
10
0
Air
Sea Water
20% LiCl
40% LiBr
Deionized water
1 hour
1 day
1 month
1 year
0
1
2
3
4
5
6
7
LOG TIME TO FAIL (sec)

Figure 7

DuPONT 707 SINGLE FIBER IN SEA WATER
EXPERIMENTAL FATIGUE DATA COMPARED TO
PREDICTION FROM CREEP RUPTURE

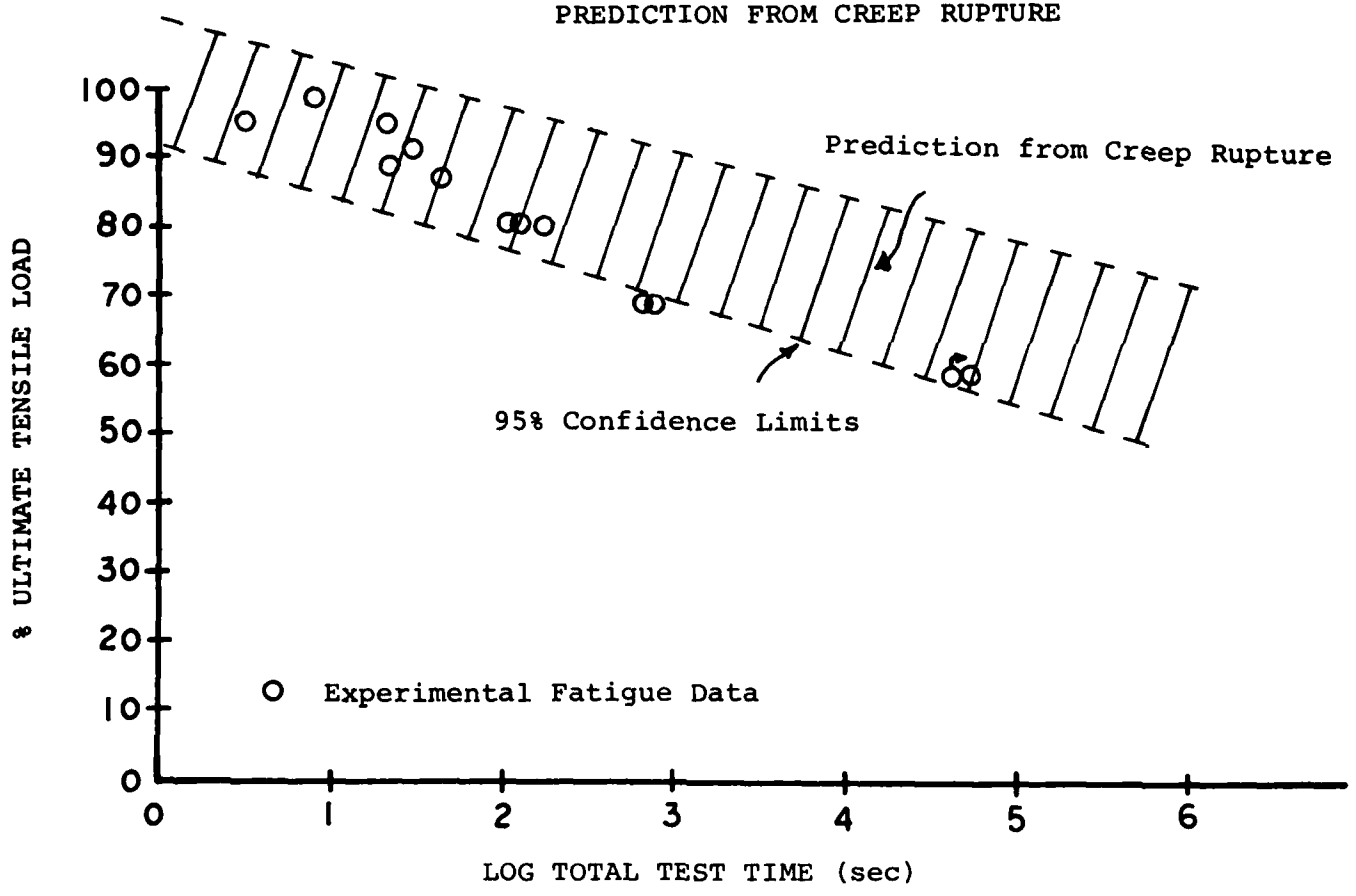

Figure 8

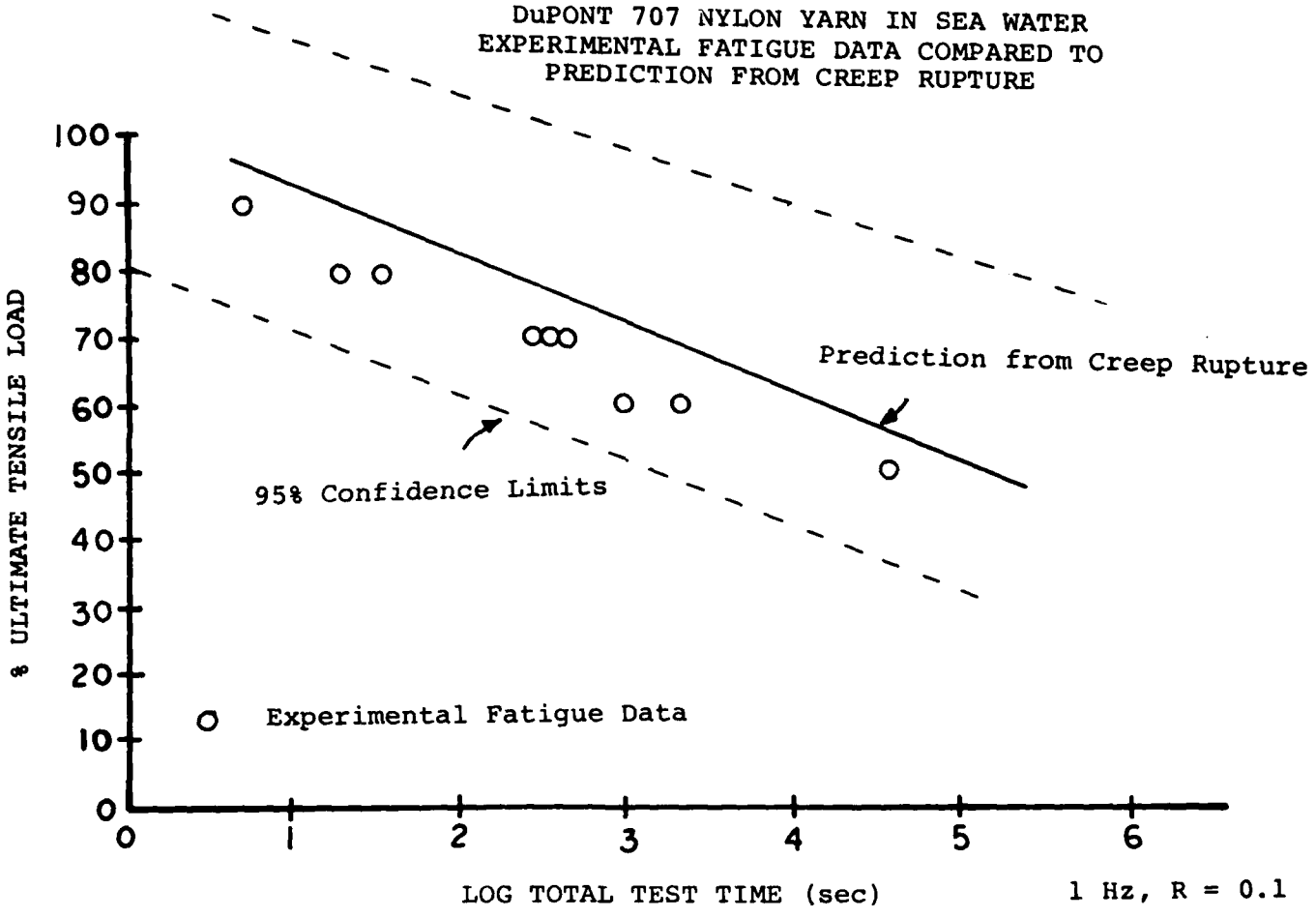
DuPONT 707 NYLON YARN IN SEA WATER
EXPERIMENTAL FATIGUE DATA COMPARED TO
PREDICTION FROM CREEP RUPTURE
% ULTIMATE TENSILE LOAD
100
90
80
70
60
50
40
30
20
10
0
0
1
2
3
4
5
6
Prediction from Creep Rupture
95% Confidence Limits
Experimental Fatigue Data
LOG TOTAL TEST TIME (sec)
1 Hz, R = 0.1

Figure 9

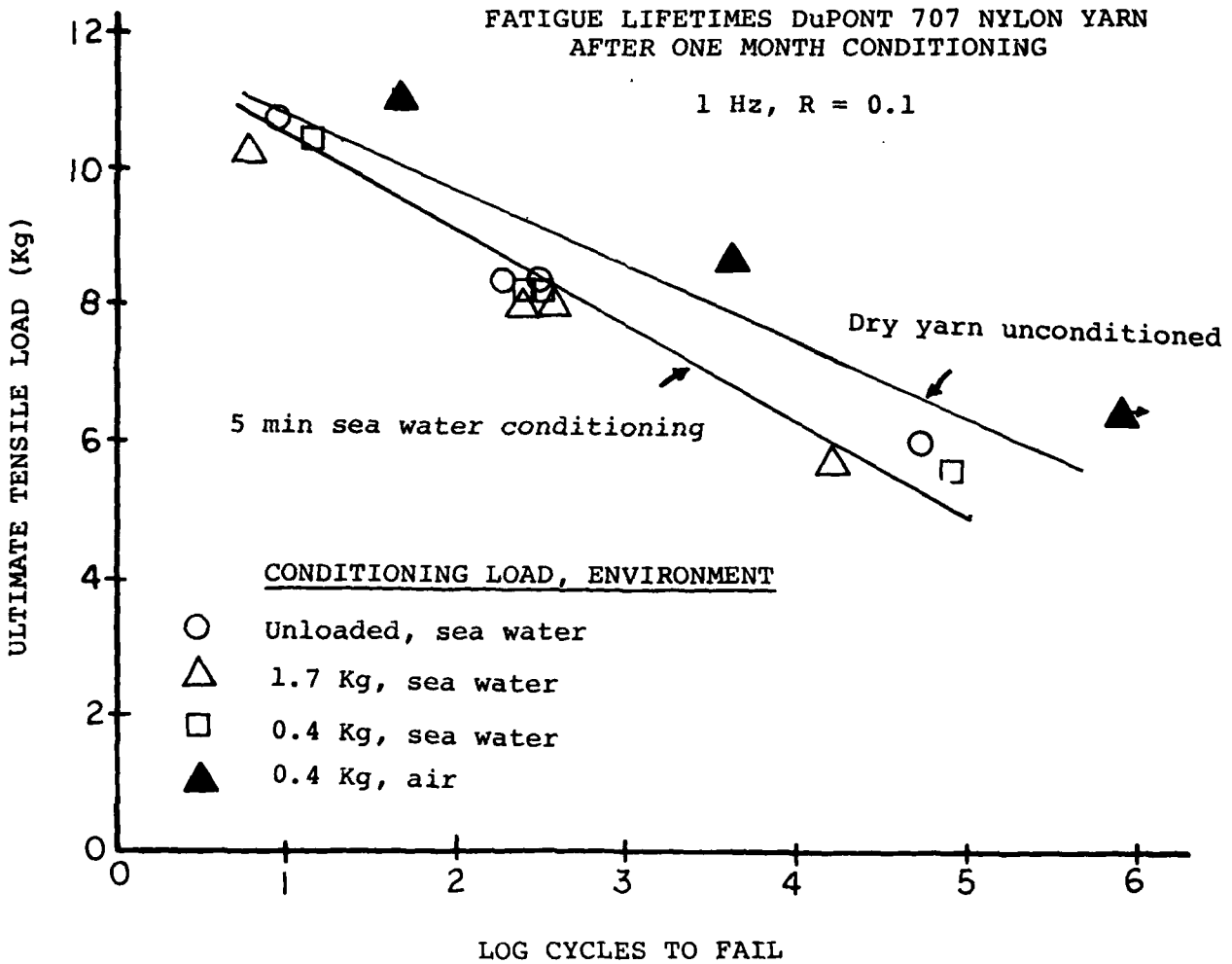
FATIGUE LIFETIMES DuPONT 707 NYLON YARN
AFTER ONE MONTH CONDITIONING
1 Hz, R = 0.1
ULTIMATE TENSILE LOAD (Kg)
LOG CYCLES TO FAIL
Dry yarn unconditioned
5 min sea water conditioning
CONDITIONING LOAD, ENVIRONMENT
Unloaded, sea water
1.7 Kg, sea water
0.4 Kg, sea water
0.4 Kg, air
0
2
4
6
8
10
12
0
1
2
3
4
5
6

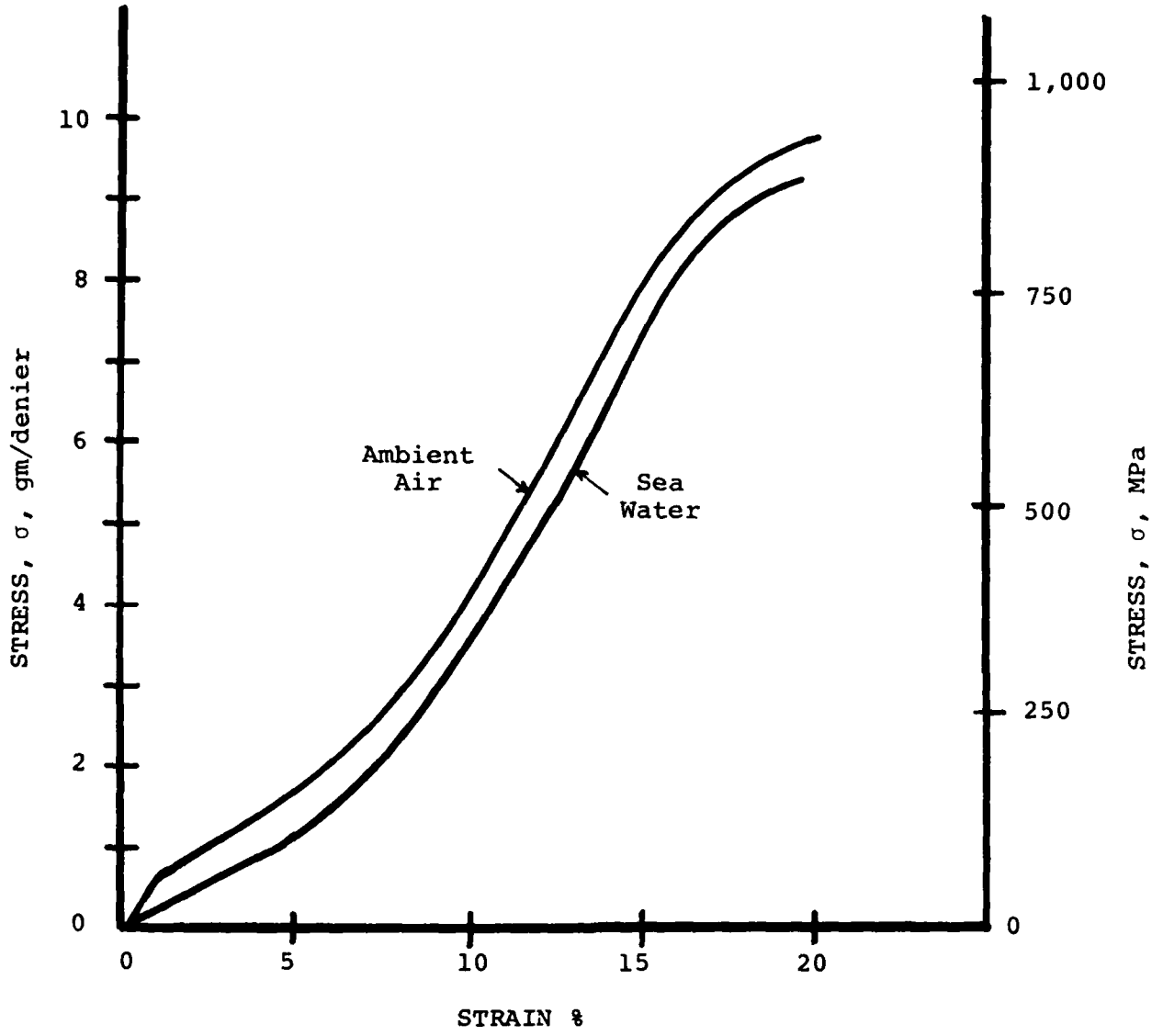

Figure 10

STRESS-STRAIN CURVES OF DUPONT 707 NYLON YARNS IN AMBIENT AIR AND SEA WATER

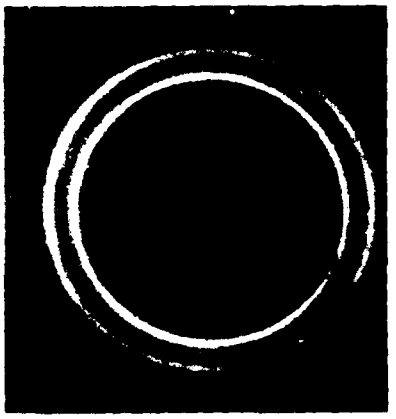

a) Machined Plaque

b) Tensile Bar

c) Drawn Tensile Bar

WIDE ANGLE X-RAY DIFFRACTION PATTERNS
OF BULK NYLON WITH INCREASING ORIENTATION

Figure 11

Figure 12

ENVIRONMENTAL STRESS CRACKING OF BULK NYLON
WITH INCREASING ORIENTATION

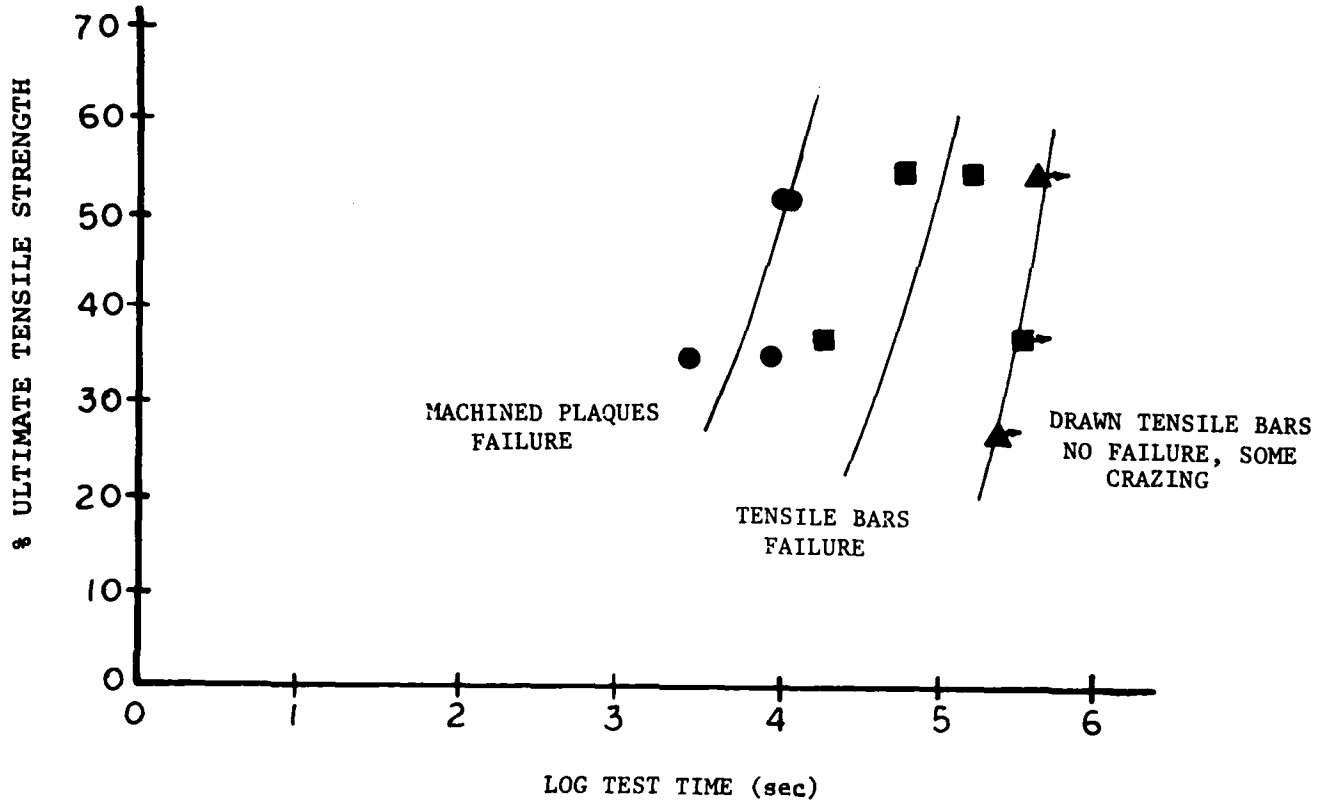

PARALLEL CRAZE STRUCTURE IN FIBER
EXPOSED TO LiCl (20% w/v)

Figure 13